APPENDIX A

Seismotectonics of the southern branch of North Anatolian Fault Zone along Bolu, Bursa, and İzmir cities and Değirmenlik (Milos) island in the Aegean Sea

GÜROL SEYİTOĞLU, KORHAN ESAT, BÜLENT KAYPAK, BEGÜM KOCA

Details of the Mudurnu Fault (MDF)

The NE-SW trending Mudurnu Fault (MDF) can be traced from southwest of Bolu to the southwest of Göynük (Figure 3). The MDF-1 lies in the NE-SW trending linear valley of Manda Dere between Sultan and Çepni villages at the southern margin of Bolu Plain towards the Saççılar village. In the northwest of Saççılar village, an elongated ridge (Mehellem Sırtı) and sharp bend of the Koca Dere are among the morphological evidence for the existence of MDF-1 (Figure A.1, Appendix C).

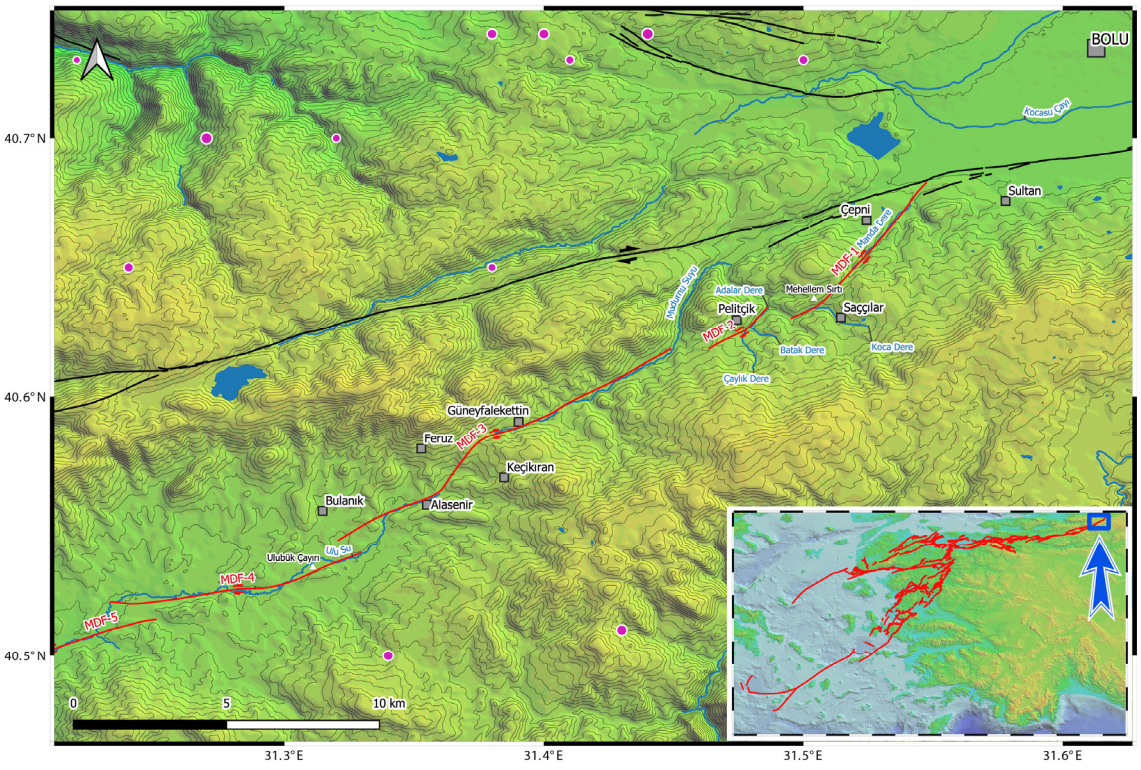

Figure A.1. The Mudurnu Fault (MDF) in the southwest of Bolu Plain. For location see inset. Black fault lines from Emre et al. (2013). Fuchsia dots with white circles are the epicenter locations of earthquakes (1900-2020, M≥3.5) from KOERI catalogue.

The en echelon, right stepping MDF-2 is located on the linear Adalar Dere valley and creates right bending of Çaylık Dere and Batak Dere at the southeast of Pelitçik. The

right stepping MDF-3 is situated in the linear Mudurnu Suyu valley, traced to Güneyfelakettin village and ends south of Bulanık village by creating a restraining bend between Feruz and Keçikıran villages. This restraining bend separates the Mudurnu Suyu flowing to the northeast and Ulu Su flowing to the southwest. At the north of Alasenir village, Ulu Su has a 1780 m right-lateral displacement along the MDF-3 (Figure A.1, Appendix C).

The MDF-4 is recognized with the right-lateral displacement of 8.40 km in Ulu Su and forming elongated ridges and sag pond (Ulubük çayırı) in the direction of east northeast – west southwest (Figures A.1 and A.2).

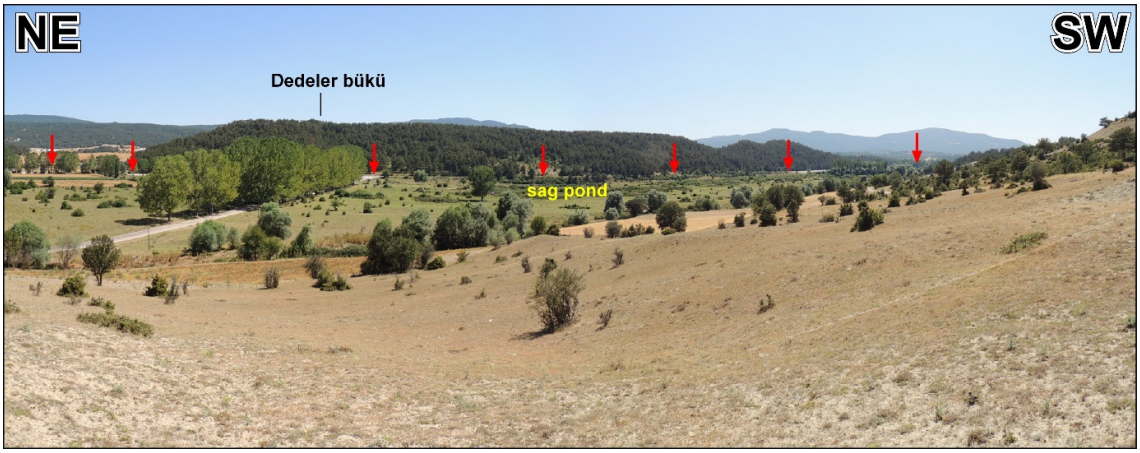

Figure A.2. Field photo of Ulubük Çayırı, a sag pond developed along segment MDF-4 (red arrows) which limits the elongated ridges such as Dedeler bükü.

The left stepping MDF-5 causes sharp termination of N-S trending valleys and ridges and creates 6.20 km right-lateral diversion in the Ulu Su and ends at the south of Munduşlar (Figure A.3, Appendix C).

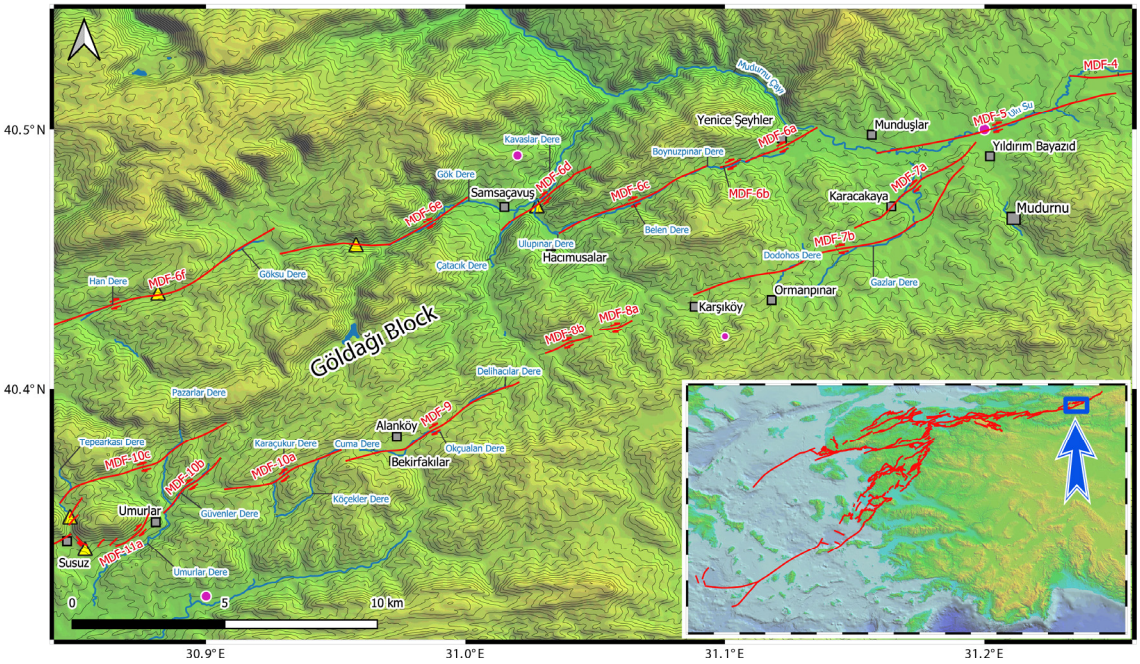

Figure A.3. The Mudurnu Fault (MDF) around northeastern part of Göldağı Block. The fault around Mudurnu were shown by Şengör et al. (1985; fig.2). Fuchsia dots with white circles are the epicenter locations of earthquakes (1900-2020, M≥3.5) from KOERI catalogue. Yellow triangles show the locations of kinematic data and field observations.

The Göldağı Block is a shuttle shape structure similar to the Almacık Block (Şengör et al., 1985; Seyitoğlu et al., 2015) and is surrounded by strike-slip faults from both northwest and southeast (Figure 3). The right stepping segments of MDF-6a_c, following the linear valleys (i.e., Boynuzpınar Dere and Belen Dere) between Yeniceşeyhler and Hacımusalar and form the northwest boundary of the Göldağı Block. In the village of Samsaçavuş, the MDF-6d, which causes the right bending of Ulupınar Dere and Çatacık Dere to be connected to Kavaslar Dere, makes a releasing stepover with the MDF-6e located inside the Gök Dere / Göynük Dere valley. This releasing stepover creates an intermountain plain where the Samsaçavuş village is located (Figure A.3, Appendix C). Highly fractured Cretaceous limestones in elongated Yapraklı Tepe and Quaternary slope debris are the indication of active faulting in this area (Figure A.4). Moreover, the segment MDF-6e provides right lateral strike-slip

kinematic data from the shear surfaces developed in the Cretaceous marl unit (Figure A.5).

Figure A.4. A) Highly fractured Cretaceous limestones in the elongated Yapraklı Tepe. **B)** Quaternary slope debris on the NW slope of Yapraklı Tepe.

The right stepping MDF-6f, which is located on the linear valleys of Göksu Dere, Han Dere and Paydos Dere, forms elongated ridge that contains Asarardı Tepe, Yükboz Tepe and Uzunburun Sırtı in the new settlement area of Göynük (Figures A.6 and A.7). The MDF-6f creates 730 m and 1400 m right-lateral displacements on the course of Çaybahçe Dere and Alaşar Dere, respectively. The southwest end of MDF-6f follows the linear valley of Göynük Çayı at the west of Kumcuk village where systematic shear fractures in the alternation of Cretaceous marl and shale provide kinematic data (Figures A.6 and A.8, Appendix C).

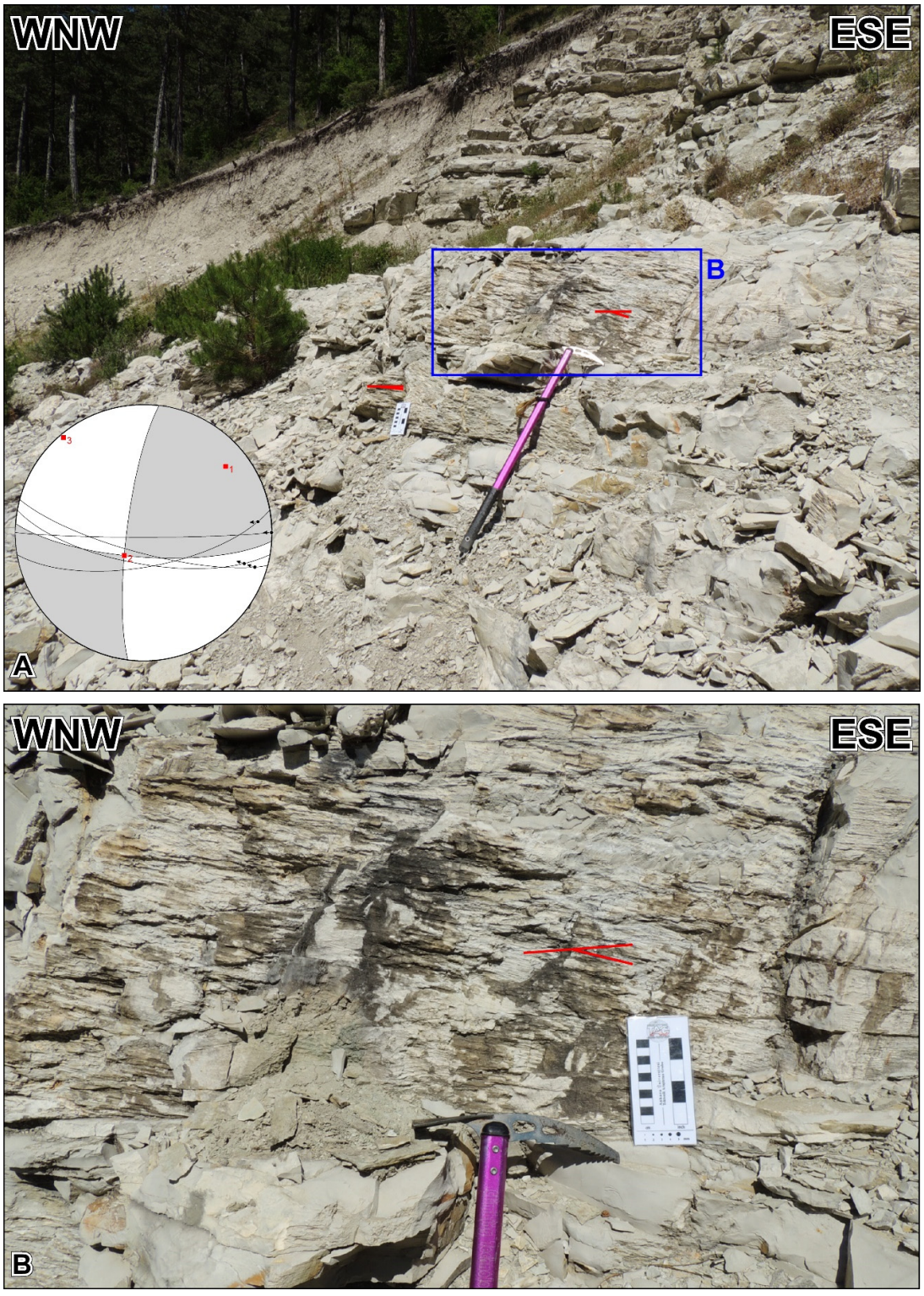

Figure A.5. A) Kinematic data from the shear fractures on the Cretaceous marls in the Göynük Dere valley along MDF-6e. **B)** Close up photo of the shear surface. The circle represents the equal area lower hemisphere spherical projection of the fault plane and slickenlines. Gray and white areas (contractional and extensional areas, respectively) are the fault plane solution obtained by kinematic analysis of the fault data. The 1, 2, and 3 indicate the orientation of kinematic (strain) axes.

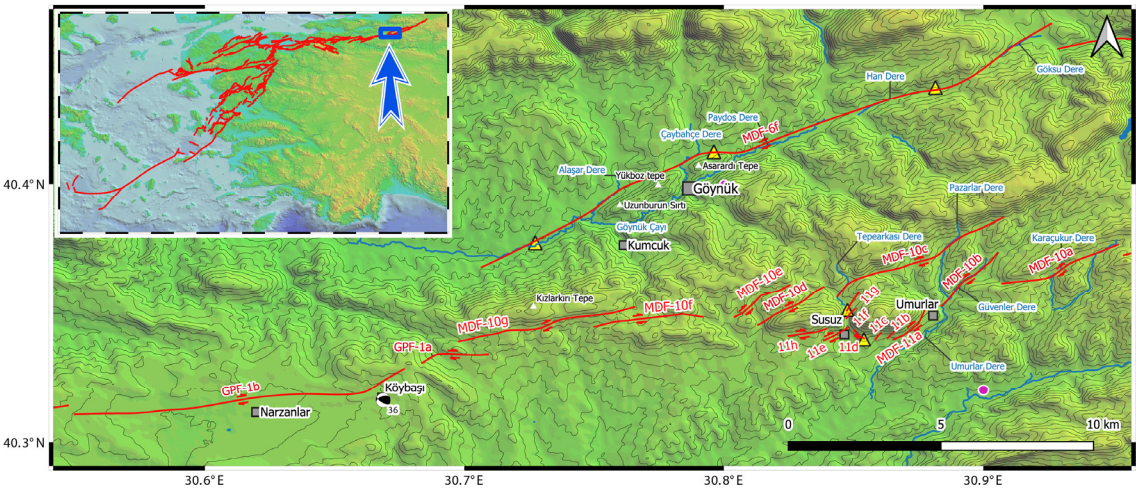

Figure A.6. The Mudurnu Fault (MDF) around southwestern part of Göldağı Block. GPF: Gölpazarı Fault. Fuchsia dots with white circles are the epicenter locations of earthquakes (1900-2020, M≥3.5) from KOERI catalogue. For details of the focal mechanism solution see Appendix B. Yellow triangles show the locations of kinematic data and field observations.

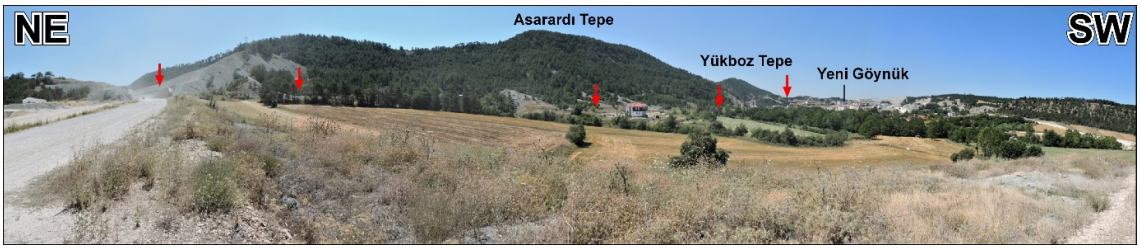

Figure A.7. The position of MDF-6f (red arrows) in the NW of elongated Asarardı and Yükboz Tepe.

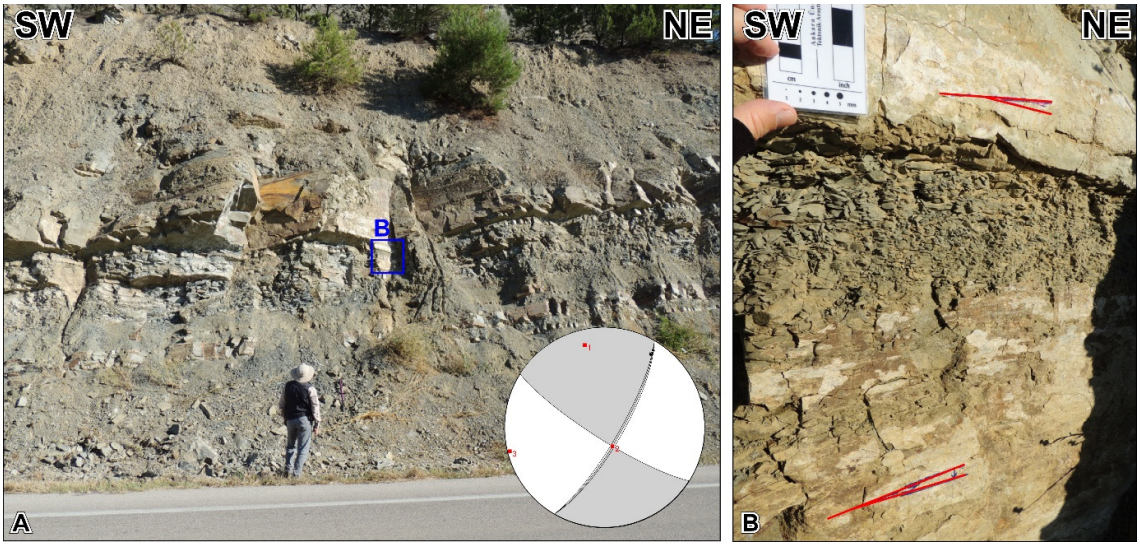

Figure A.8. A) Systematic shear fractures in the Cretaceous marl and shale alternation provides kinematic data in the linear valley where MDF-6f is located. **B)** Close-up view of the shear fractures. The circle represents the equal area lower hemisphere spherical projection of the fault plane and slickenlines. Gray and white areas (contractional and extensional areas, respectively) are the fault plane solution obtained by kinematic analysis of the fault data. The 1, 2, and 3 indicate the orientation of kinematic (strain) axes.

The MDF-7a_b forming the southeast boundary of Göldağı Block extends from Yıldırım Bayazıt settlement to Karşıköy (Figure A.3). The NE-SW trending MDF-7a creates 450 m and 360 m right-lateral displacements on the semi-parallel stream channels at the north of Karacakaya. The MDF-7b has the right-lateral displacements of 2850 m and 670 m on Gazlar Dere and Dodohos Dere at the north of Ormanpınar. These right-lateral displacements on the semi-parallel stream channels are strong morphological indicators for the segments MDF-7a_b. After short en echelon segments (MDF-8a_b), the MDF-9, which is located on mainly the linear valley of Delihacılar Dere, passes between Bekirfakılar and Alan villages and controls the positions of Okçualan Dere and Cuma Dere (Figure A.3). The NE-SW trending en echelon segments (MDF-10a_d) generally located on the linear valleys and cause right bending of streams (i.e., Karaçukur and Köçekler Dere along MDF-10a; Güvenler Dere along MDF-10b; Pazarlar Dere and Tepearkası Dere along MDF-10c) (Figure A.6, Appendix C). The en echelon NE-SW trending MDF-11a_c limits west and south of Aktepe where travertines occur in the releasing offset between MDF-11e and MDF-11c at the east of Susuz (Figure A.9).

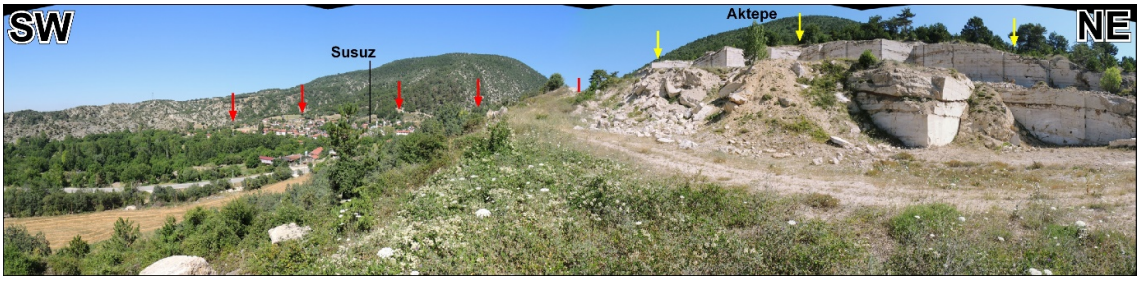

Figure A.9. Travertines in the east of Susuz. Red arrows indicate position of MDF-11e. Yellow arrows show the possible location of NW-SE trending normal faults.

Several en echelon NE-SW trending segments (MDF-10c_e and MDF-11f_g) are recognized by using morphological features (i.e., linear valleys) in the north of Susuz. One of them, MDF-11g, provides kinematic data inside a quarry (Figure A.10).

The southeastern border of the Göldağı Block is completed with the segments MDF-10f_g which have ENE-WSW trend between Kızlarkırı Tepe and Susuz. (Figure A.6, Appendix C).

Figure A.10. A) Panoramic photo in the quarry, north of Susuz. **B)** Systematic shear fractures trending NE-SW. **C)** Close-up view of the kinematic data. **D)** Right lateral strike-slip kinematic data from the shear surfaces. The length of ice axe is 80 cm. The circle represents the equal area lower hemisphere spherical projection of the fault plane and slickenlines. Gray and white areas (contractional and extensional areas, respectively) are the fault plane solution obtained by kinematic analysis of the fault data. The 1, 2, and 3 indicate the orientation of kinematic (strain) axes.

Details of the Gölpazarı Fault (GPF)

Gölpazarı Fault (GPF) is separated from Mudurnu Fault (MDF) with left stepping GPF-1a at the northeast of Köybaşı (Figure 3). The GPF-1b passes at the north of Köybaşı and Narzanlar. Its location is determined by using bending of streams and spring locations in a flat topography (Figure A.6, Appendix C). The GPF-1c creates right

bending of Kavşak Dere at the south southwest of Hacıaliler between Erenler Tepe and Günel Tepe (Figure A.11).

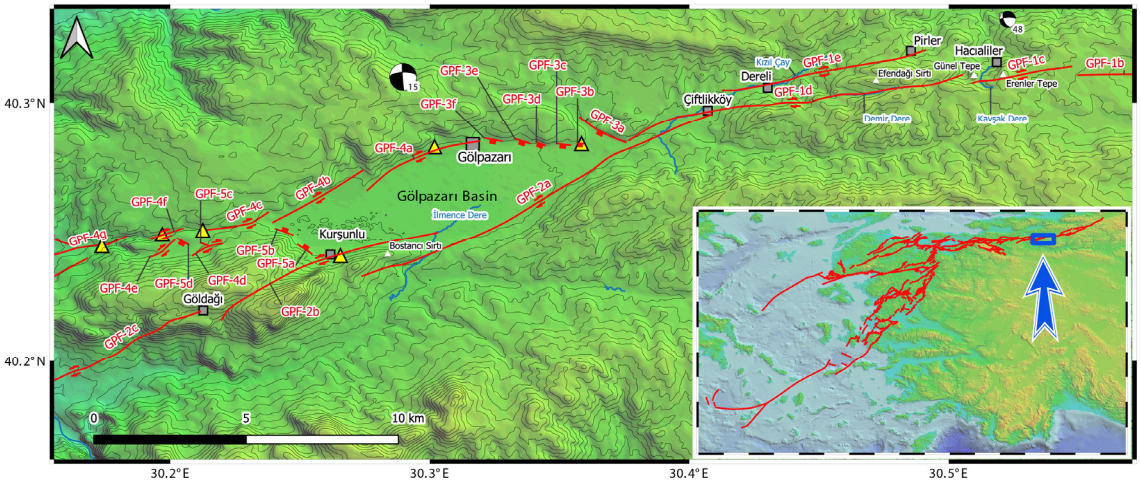

Figure A.11. Gölpazarı Fault (GPF) and the pull-apart basin. The structural data locations (yellow triangles) from Gürbüz and Seyitoğlu (2014) and this paper. For details of the focal mechanism solution see Appendix B. Yellow triangles show the locations of kinematic data and field observations.

The GPF-1d is one of the longest segments and mainly follows the linear valley of Demir Dere at the south of elongated ridge of Efendağı Sırtı and creates a 615 m right lateral displacement on the course of Kızıl Çay at the northeast of Gölpazarı pull-apart basin (Gürbüz and Seyitoğlu, 2014) (Figure A.11). The semi-parallel segment GPF-1e lies between Çiftlik and Pirler villages and 1750 m right lateral shifting on route of Kızıl Çay is measured at the north of Dereli (Figure A.11, Appendix C).

The segment GPF-2a somewhat corresponds to the Kurşunlu-Dereli segment of Gürbüz and Seyitoğlu (2014) which limits southeastern margin of Gölpazarı pull-apart basin (Figures A.11 and A.12).

Figure A.12. A) The view of Gölpazarı pull-apart basin from west to southeast. GPF-2a and 2b are shown as red arrows. **B)** The view from southwest to northeast. The red arrows near Kurşunlu indicate GPF-2b and the red arrows in the other side of the pull-apart basin are GPF-4a and 4b. The yellow arrows indicate normal faults, GPF-3b_f.

The GPF-2a cause 970 m right lateral displacement on the course of İlmence Dere due to Bostancı Sırtı which may be evaluated as a shutter ridge. The en echelon GPF-2b passes through Kurşunlu village and follows the linear valley towards Göldağı village. The structural data from the fault surface is reported from this segment (Gürbüz and Seyitoğlu, 2014). The right stepping GPF-2c creates a releasing stepover where the village of Göldağı is located at the northern corner of the small plain (Figure A.11, Appendix C).

The southwestern continuation of GPF-2c diverts the route of Sakarya River at the east of Selbükü (Figure A.13). The northeast margin of the Gölpazarı pull-apart basin is limited by en echelon normal faults (GPF-3a_f) (Gürbüz and Seyitoğlu, 2014)

(Figure A.11). The northwest margin of Gölpazarı pull-apart is limited by en echelon segments of GPF-4a_b having structural data presented in Gürbüz and Seyitoğlu (2014). The focal mechanism solution of the seismic event #15_1999.09.13 (Md=5.8) confirms the right-lateral strike-slip nature of the segments (Appendix B). The short en echelon segments of GPF-4c, GPF-4f and GPF-4g provide a connection between Gölpazarı pull-apart basin and the Üyük pull-apart basin (Figures A.11 and A.13). The GPF-4c provides shear surfaces having kinematic data (Figure A.14).

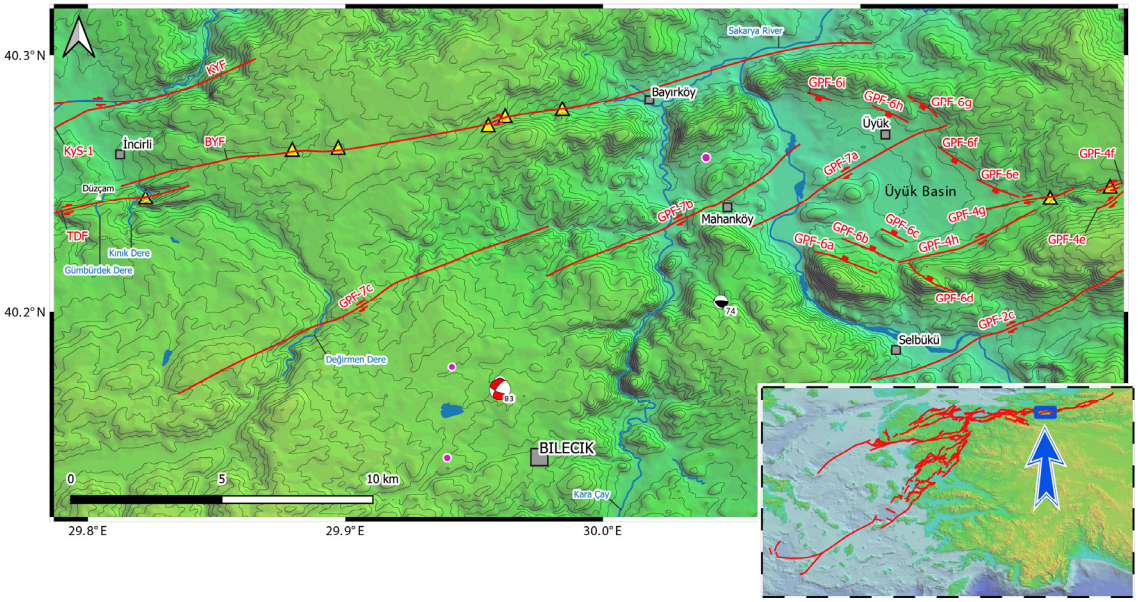

Figure A.13. A releasing stepover between Bayırköy Fault (BYF) and Gölpazarı Fault (GPF) and the position of Üyük basin. Fuchsia dots with white circles are the epicenter locations of earthquakes (1900-2020, M≥3.5) from KOERI catalogue. For details of the focal mechanism solution see Appendix B. Yellow triangles show the locations of kinematic data and field observations.

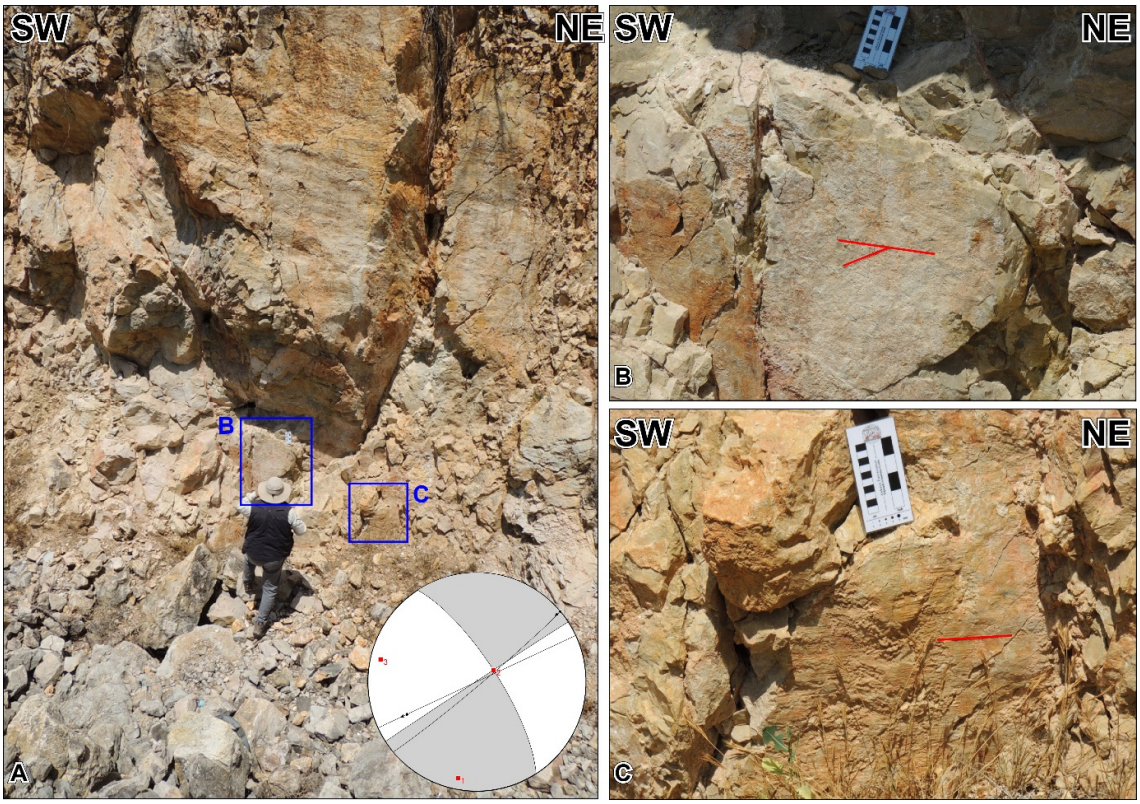

Figure A.14. A) Shear surface along GPF-4c between Gölpazarı and Üyük pull-apart basins. **B** and **C)** Close-up view of the kinematic data. The circle represents the equal area lower hemisphere spherical projection of the fault plane and slickenlines. Gray and white areas (contractional and extensional areas, respectively) are the fault plane solution obtained by kinematic analysis of the fault data. The 1, 2, and 3 indicate the orientation of kinematic (strain) axes.

The southeastern part of Üyük basin is developed between NE-SW trending right-lateral GPF-4g_h and GPF-7a_b. Its northeast and southwest margins are limited by NW-SE trending normal fault segments (GPF-6a_f) (Figure A.13). The strike-slip fault (GPF-7a), dividing the Üyük basin, creates a 1265 m right lateral shift on the route of Sakarya River at the east southeast of Mahanköy (Figure A.13, Appendix C). The en echelon GPF-7b displaces right-laterally both Sakarya River (610 m) and Kara Çay (425 m). Another important right-lateral shift (1580 m) on the course of Değirmen Dere are measured along the segment GPF-7c (Figure A.13). The focal mechanism solution of seismic event #83_2011.07.11 (ML=4.6) supports right-lateral strike-slip characters of the segments in this area (Figure A.13, Appendix B).

A releasing step over between GPF-4g_h and Bayırköy Fault (BYF) (see below) created Üyük pull-apart basin which is also dissected by the NE-SW trending segments (GPF-7a_c) which displaced the routes of major river/streams right-laterally such as Sakarya River, Kara Çay and Değirmen Dere (Figures 3, A.13, A.15 and Appendix C).

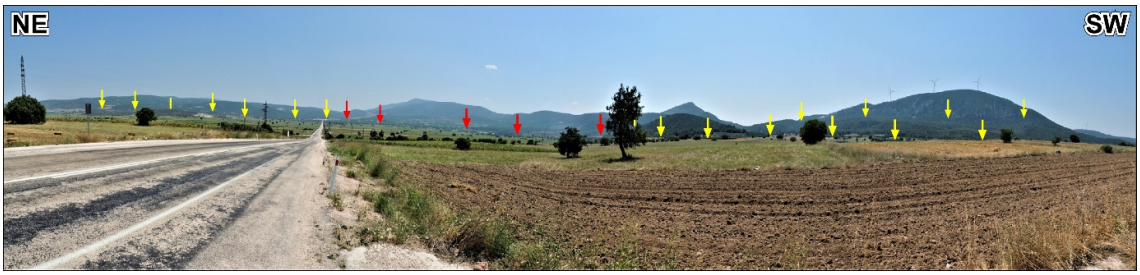

Figure A.15. Panoramic view of Üyük pull-apart basin. Yellow arrows on the right are the normal fault segments GPF-6a_c. The yellow arrows on the left represent position of normal fault segments GPF-6e_f. The red arrows in the middle are the right lateral strike-slip segments of GPF-4g_h. See Figure A.13 for the map.

Details of Bursa and Yenişehir faults

The Bayırköy Fault (BYF) is the important right-lateral strike-slip structure that has a linkage role between the Yenişehir and Gölpazarı pull-apart basins (Figure 3, A.13). It causes a 2.93 km right-lateral displacement on the Sakarya River (Seyitoğlu et al., 2016) and can be followed to the south of İncirli as a single line (Figures A.13 and A.16) via Sarmaşık village where right lateral strike-slip kinematic data obtained from shear surface (Figure A.17).

Figure A.16. The Bayırköy Fault in the field, looking NE. This fault diverts Sakarya River and Kara Çay. See Figure A.13 for photo location.

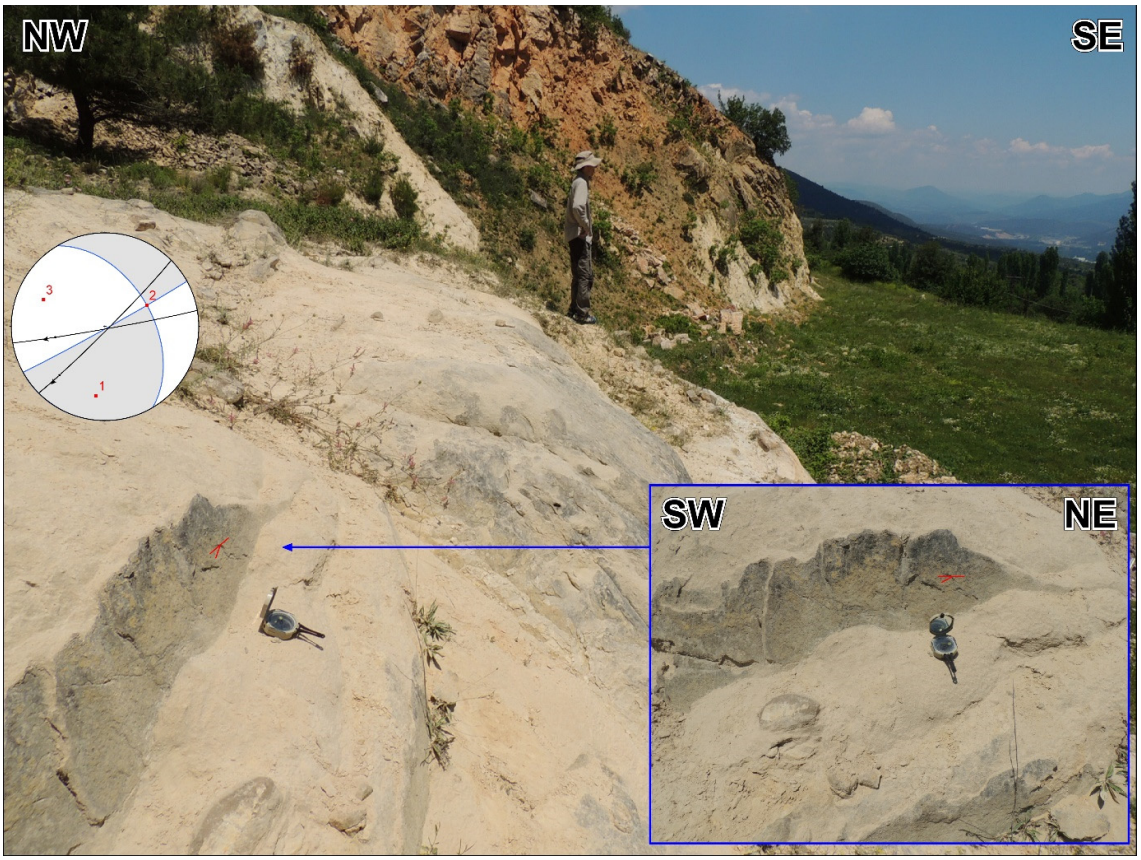

Figure A.17. A shear surface and right lateral kinematic data along the BYF in the SW exit of Sarmaşık village. The circle represents the equal area lower hemisphere spherical projection of the fault plane and slickenlines. Gray and white areas (contractional and extensional areas, respectively) are the fault plane solution obtained by kinematic analysis of the fault data. The 1, 2, and 3 indicate the orientation of kinematic (strain) axes.

The en echelon Toprakdere Fault (TDF) has well developed fault surfaces in the Kınık Dere valley and creates several right-lateral displacements of the stream channels

such as 500 m on Kınık Dere, 170 m south of Düzçam, 180 m on Gümbürdek Dere, 980 m on Yavğılı Dere (Figures A.13, A.18, and Appendix C).

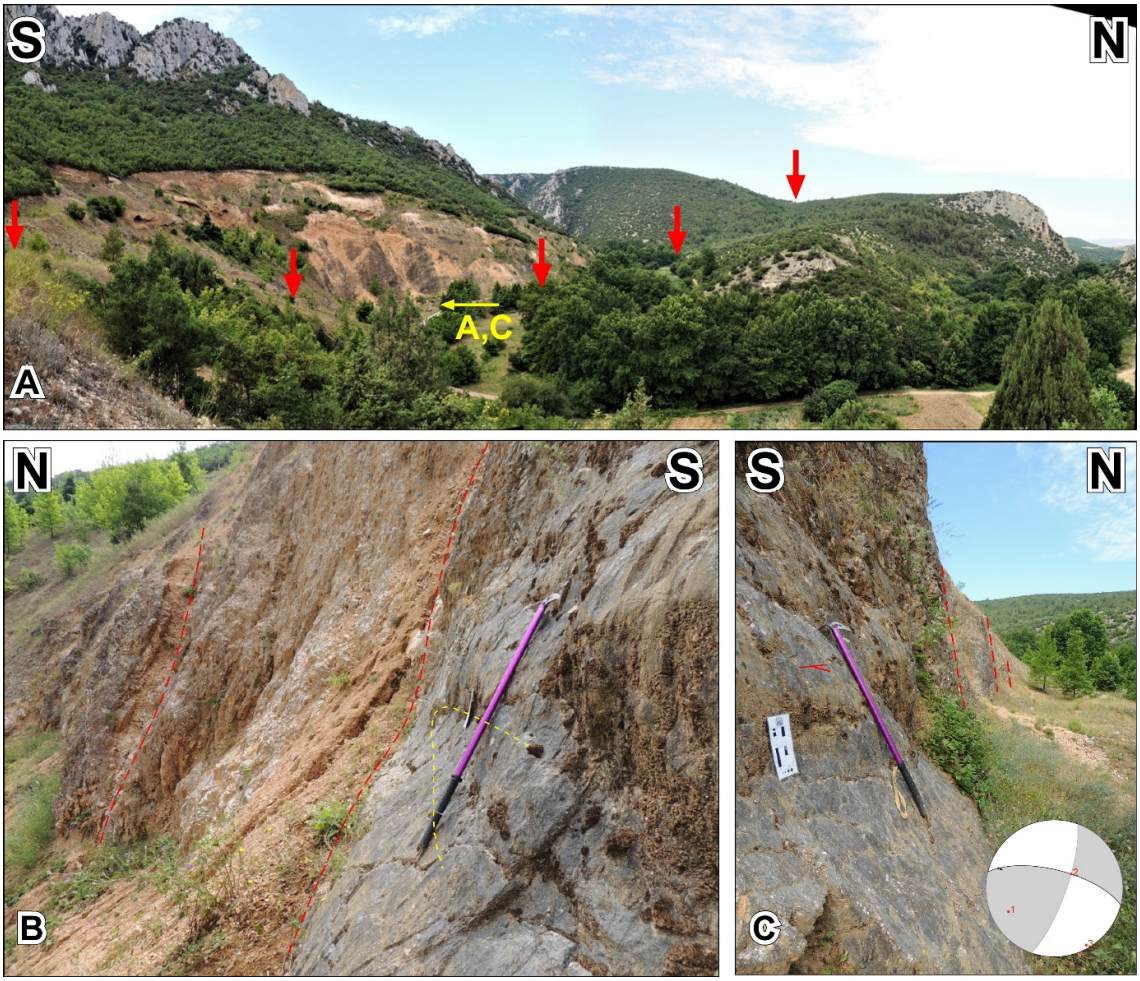

Figure A.18. The Toprakdere Fault (TDF) in the Kınık Dere valley. See Figure A.5 for location. **A)** The red arrows show the position of TDF and the right-laterally displaced Kınık Dere. **B)** Close-up view of the fault surface. The carrot structure is marked with yellow dashed line. **C)** The slickenlines on the fault surface. The circle represents the equal area lower hemisphere spherical projection of the fault plane and slickenlines. Gray and white areas (contractional and extensional areas, respectively) are the fault plane solution obtained by kinematic analysis of the fault data. The 1, 2, and 3 indicate the orientation of kinematic (strain) axes (after Seyitoğlu et al., 2021).

Eastern margin of the Yenişehir pull-apart basin is composed of the NE-SW trending Subaşı (SBF) and Boğazköy (BZF) faults (Figures 3 and A.19). The right-lateral strike-slip kinematic data from the fault surfaces of Subaşı and Boğazköy were obtained (Seyitoğlu et al., 2021).

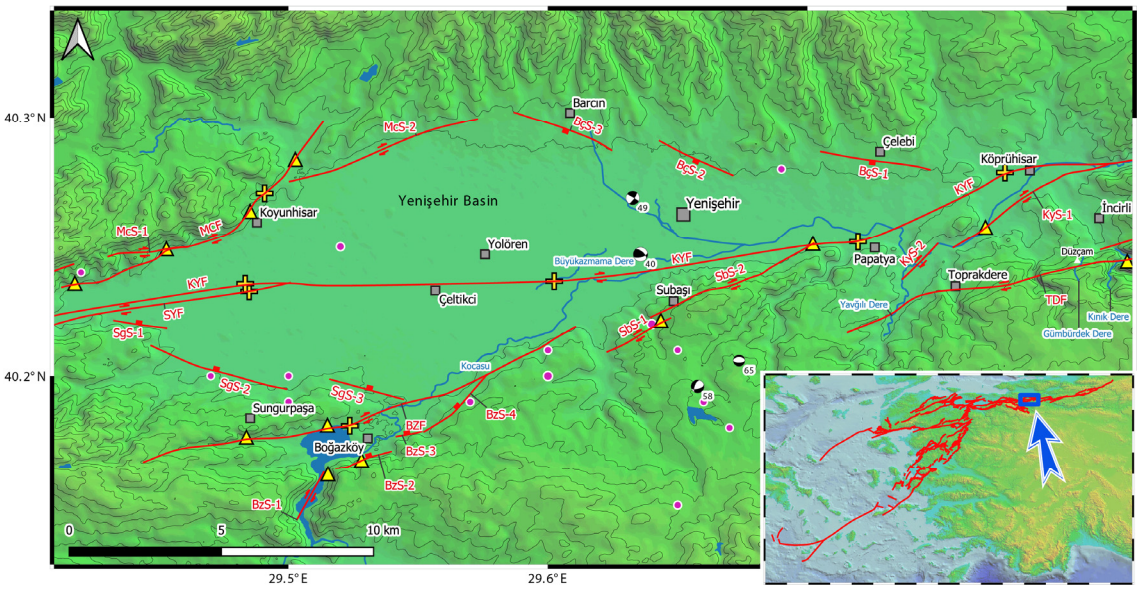

Figure A.19. The Yenişehir pull-apart basin and the cross basin Kayapa-Yenişehir Fault (KYF). The KYF right laterally displaced both Büyükazmama Dere and Kocasu. Fuchsia dots with white circles are the epicenter locations of earthquakes (1900-2020, M≥3.5) from KOERI catalogue. For details of the focal mechanism solution see Appendix B. The structural data locations (yellow triangles) and seismic reflection data locations (yellow plus signs) from Seyitoğlu et al., (2021). See previous studies (Yılmaz and Koral, 2007; Emre et al., 2013; 2018; Selim et al., 2013) for comparison. McS: the segments of Marmaracık Fault (MCF); BçS: the segments of Barçın-Çelebi normal fault; TDF: Toprakdere Fault; BYF: Bayırköy Fault; KyS: segments of Kayapa-Yenişehir Fault (KYF); SbS: the segments of Subaşı Fault (SBF); SgS: the segments of Sungurpaşa Fault (SGF); SYF: Seymen Fault; BzS: the segments of Boğazköy Fault (BZF).

Moreover, seismic reflection data confirmed the position of Boğazköy Fault. The northeast and southwest margins of the Yenişehir pull-apart basin is bounded by the WNW-ESE trending Barçın-Çelebi and Sungurpaşa normal faults dipping SW and NE respectively. The segments of both Barçın-Çelebi and Sungurpaşa faults are determined based on morphology (Figure A.19).

The western margin of Yenişehir pull-apart basin is composed of NE-SW trending Marmaracık (MCF) and Sarı Tepe (STF) faults. The structural data indicate that faults are right-lateral strike-slip in nature. In the north of Koyunhisar, a seismic reflection section proves the position of MCF (Seyitoğlu et al., 2021) (Figure A.19).

The northern margin of Bursa-east pull-apart basin is limited by WNW-ESE trending, SW dipping Barakfakıh normal fault as indicated by the focal mechanism solution of the seismic event #77_2010.09.08 (Md=3.2) (Figures 3, A.20 and Appendix B). It creates distinguished topographical differences and some of the segments separated by left-lateral transfer faults. The southwestern margin of Bursa-east pull-apart is also limited by the NW-SE trending NE dipping Bursa Fault.

It can be interpreted as a part of re-activated Bursa detachment fault which is responsible for the exhumation of Uludağ core complex (Seyitoğlu et al., 2021; Seyitoğlu and Esat, 2022b). The normal fault related focal mechanism solutions of the seismic events #105_2019.11.16 (Ml=3.0) and #106_2019.11.17 (Ml=3.2) demonstrate that the segments (BuS-1, BuS-2, BuS-3) of Bursa Fault is active (Figure A.20).

The Yıldırım Fault (YDF) limits the eastern margin of Bursa-east pull-apart basin (Figure 3). It is recognized by a sudden 1.2 km right shifting of Kaplıkaya Dere (Seyitoğlu et al., 2016) and creates left bend of Deliçay (Figure A.20). The YDF is also confirmed by a seismic reflection section (Seyitoğlu et al., 2021). The eastern margin of Bursa-east pull-apart basin is composed of right-lateral faults of Gümüştepe (GTF) and Çekirge-Kazıklı (ÇKF) faults (Figure A.20). The GTF creates 1 km and 2.3 km right lateral displacement on the Çalık Dere and Nilüfer Çay respectively (Figure A.21). Maltepe plays a role of shutter ridge. The en echelon ÇKF can be followed on the northwest slopes of Maltepe and controls the position of hot springs in Çekirge where the seismic reflection studies confirmed its location (Seyitoğlu et al., 2021). The ÇKF mainly controls the route of Nilüfer Çayı in the Bursa Plain and reached to the northwest of Kazıklı village (Figures 3, A.20, and A.21). In this location, the focal

mechanism solution of seismic event #86_2016.06.07 (ML=4.6) confirms the right-lateral faulting (Figure A.20, Appendix B).

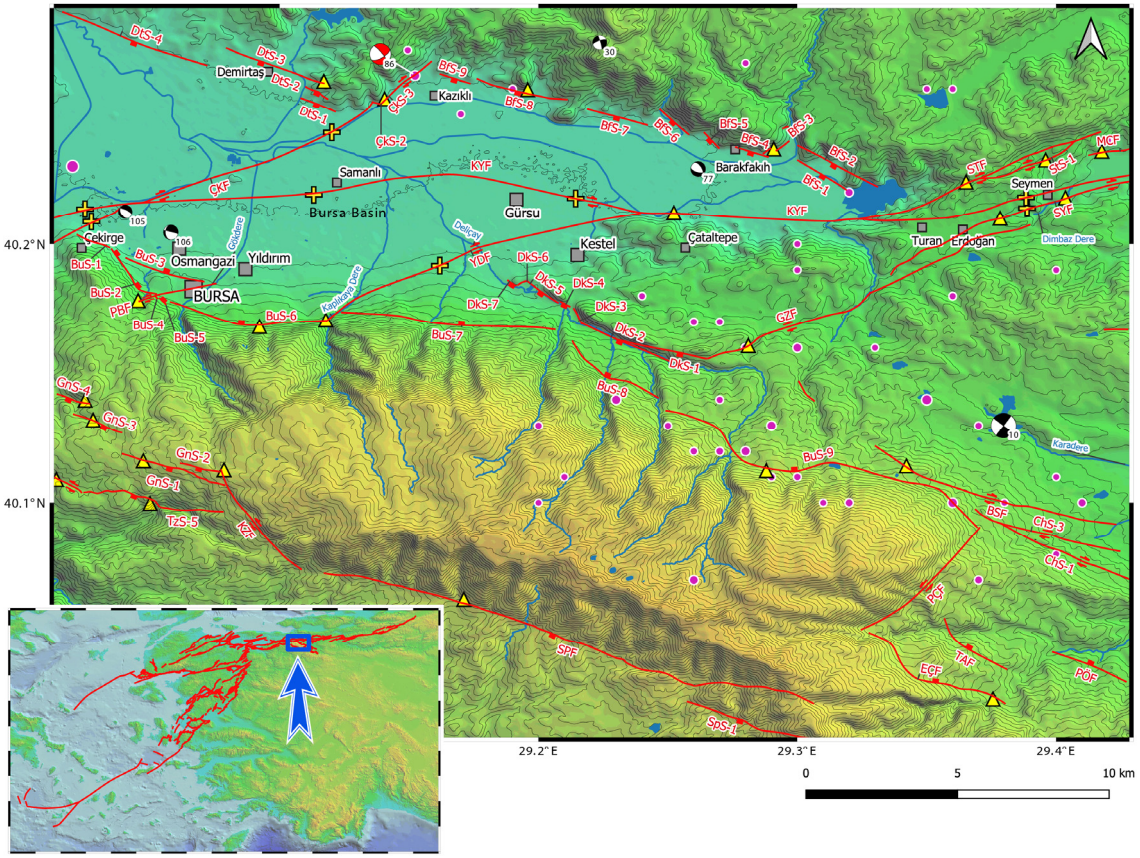

Figure A.20. The Bursa-east pull-apart basin and cross-cutting Kayapa-Yenişehir Fault (KYF). Fuchsia dots with white circles are the epicenter locations of earthquakes (1900-2020, M≥3.5) from KOERI catalogue. For the focal mechanism solutions see Appendix B. The structural data locations (yellow triangles) and seismic reflection data locations (yellow plus signs) from Seyitoğlu et al. (2021). See previous studies (Emre et al., 2013; 2018; Selim et al., 2013) for comparison. MCF: Marmaracık Fault, StS: the segments of Sarı Tepe Fault (STF), SYF: Seymen Fault, BfS: the segments of Barakfakıh Fault (BFF), GZF: Gözede Fault, DkS: The segments of Derekızık Fault (DKF), BuS: the segments of Bursa Fault (BUF), YTF: Yıldırım Fault, ÇkS: the segments of Çekirge-Kazıklı Fault (ÇKF), DtS: the segments of Demirtaş Fault (DTF), KZF: Kirazlı Fault, SPF: Soğukpınar Fault, EÇF: Elmaçayır Fault, TAF: Turgutalp Fault; PÖF: Paşaören Fault; PÇF: Pelitçayı Fault; ChS: the segments of Cerrah Fault (CHF) of the Eskişehir Fault Zone; BSF: Babasultan Fault of Eskişehir Fault Zone.

The northeast margin of Bursa-west pull-apart basin is limited by the Demirtaş Fault (DTF) (Figure 3). This NW-SE trending, SW dipping normal fault has three segments and defined by using morphology (Figure A.20). The Çalı-Tahtalı Fault (ÇTF) limits the southwest margin of Bursa-west basin (Figure A.21) and structural data derived from its footwall (Seyitoğlu et al., 2021).

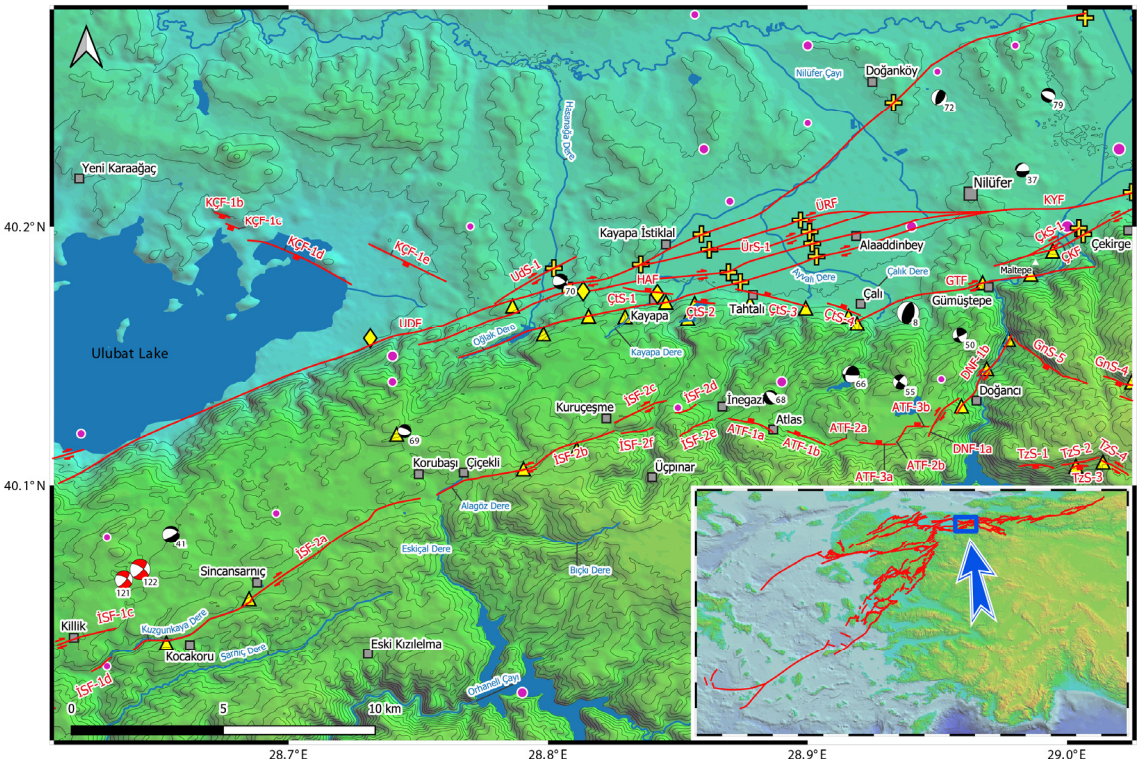

Figure A.21. The Ulubat-Doğanköy Fault (UDF) between Bursa-west and Ulubat pull-apart basins and southwest end of the cross basin Kayapa-Yenişehir Fault (KYP). Fuchsia dots with white circles are the epicenter locations of earthquakes (1900-2020, M≥3.5) from KOERI catalogue. For the focal mechanism solutions see Appendix B. The structural data locations (yellow triangles) and seismic reflection data locations (yellow plus signs) from Seyitoğlu et al. (2021). The yellow rhombic signs are paleoseismological trench locations of Özaksoy (2018) and Karabacak et al. (2021a). See previous studies (Emre et al., 2013; 2018; Selim et al., 2013) for comparison. KYF: Kayapa-Yenişehir Fault; UDF: Ulubat-Doğanköy Fault; HAF: Hasanağa-Alaaddin Fault; ÜrS: the segments of Ürünlü Fault (ÜRF); ÇkS: the segments of Çekirge-Kazıklı Fault (ÇKF); GTF: Gümüştepe Fault; ÇtS: the segments of Çalı-Tahtalı Fault (ÇTF); DNF: Doğancı Fault; ATF: Atlas Fault; İSF: İnegazi-Sincansarnıç Fault; KÇF: Karaağaç Fault.

The northwest margin of Bursa-west basin is bounded by Ulubat-Doğanköy Fault (UDF) (Figure 3). The UDF creates topographical differences on the southeast side of Ulubat Lake (Figures A.21 and A.22).

Figure A.22. Distinctive morphology of the Ulubat-Doğanköy Fault (UDF) at the southeast of Ulubat Lake.

The elongated ridge displacement (131 m), the shifting of Hasanağa Dere (135 m), the stream channel displacement at Kayapa İstiklal (193 m), and the dislocation of Ayvalı Dere (4.93 km) all indicate the right-lateral movement on the UDF. Its location is confirmed by the six different seismic reflection sections (Figure A.21) (Seyitoğlu et al., 2021). The focal mechanism solution indicating SE dipping normal fault with right-lateral component of the seismic event #70_2009.06.20 (Md=3.3) may be related to the UDF. The focal mechanism solution showing nearly pure normal faulting of the seismic event #69_2009.04.25 (Md=3.3) is kinematically concordant with NE-SW trending right lateral strike-slip faulting. The reverse / thrust fault related focal mechanism solution of the seismic event #8_1983.02.01 (Md=4.8) could be related to the Gümüştepe Fault (GTF) where Maltepe shutter ridge is created in the restraining stepover with the Çekirge Fault (ÇKF) (Figure A.21, Appendix B).

More important finding in the Yenişehir, Bursa-east, and Bursa-west pull-apart basins is the determination of cross-basin Kayapa-Yenişehir Fault (KYF). The northeast end of KYF is nearly parallel to the BYF and TDF in the northeast corner of Yenişehir pull-apart basin (Figure 3). It is confirmed by the seismic reflection sections in Köprühisar, Papatya, Çeltikçi, and Yolören (Seyitoğlu et al., 2021). In the south southwest of Yenişehir, the KYF creates both 2.24 km right-lateral displacement on Kocasu and 950 m right-lateral shift on the Büyükazmama Dere (Figure A.19). In the southwest corner of Yenişehir pull-apart basin, a 650 m right-lateral dislocation on Dimbaz Dere is measured at the northeast of Seymen village. The semi-parallel Seymen Fault (SYF) (Figures A.19, A.20 and A.23) presents structural data between Erdoğan and Seymen, and its continuation can be followed in the seismic reflection sections (Seyitoğlu et al., 2021).

The KYF turns to the east-west direction around Turanköy and become obvious with the fault surfaces parallel to the road D200 at the mountain-piedmont junction at the northwest of Çataltepe (Figures A.20 and A.24). Towards west, the continuation of KYF in the Bursa Plain is determined by several seismic reflection sections such as Gürsu, Samanlı, Paşa Çiftliği, Alaaddinbey, Kayapa Zafer. The outcrops of KYF shear zones can be seen in the valley of Kayapa Dere which is diverted 1230 m right-laterally (Figures A.21 and A.25). After observations of the shear zone in the quarries, the KYF ends in the linear valley of Oğlak Dere which is parallel to the UDF (Figure A.21). The KYF is the longest right-lateral strike-slip fault that is observable surface and subsurface data and cross-cutting the Yenişehir, Bursa-east, Bursa-west pull-apart basins (Seyitoğlu et al., 2021) (Figure 3).

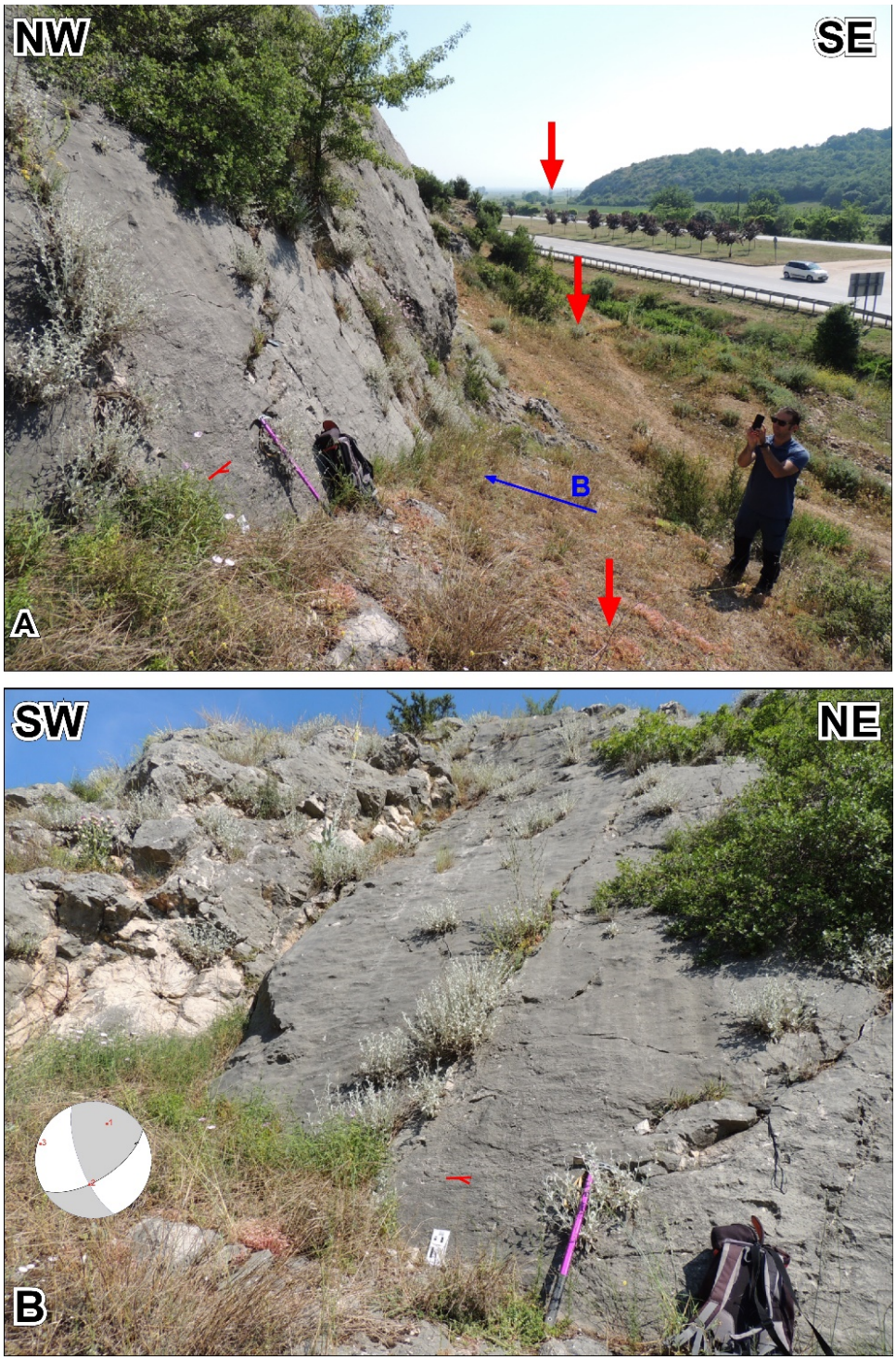

Figure A.23. A) The fault surface of Seymen Fault (SYF) on the road of Seymen village (see Figure A.20). This fault enters to the Yenişehir pull-apart basin (red arrows) which is parallel to the Kayapa-Yenişehir Fault (KYF). **B)** The fault surface in different perspective. The circle represents the equal area lower hemisphere spherical projection of the fault plane and slicken-lines. Gray and white areas (contractional and extensional areas, respectively) are the fault plane solution obtained by kinematic analysis of the fault data. The 1, 2, and 3 indicate the orientation of kinematic (strain) axes (after Seyitoğlu et al., 2021).

Figure A.24. A) The fault surface of cross-basin Kayapa-Yenişehir Fault (KYF) on the D200 Bursa-Ankara road at the northeast of Çataltepe (Figure A.20). **B)** The fault surface and slicken-lines in different perspective. The circle represents the equal area lower hemisphere spherical projection of the fault plane and slicken-lines. Gray and white areas (contractional and extensional areas, respectively) are the fault plane solution obtained by kinematic analysis of the fault data. The 1, 2, and 3 indicate the orientation of kinematic (strain) axes (after Seyitoğlu et al., 2021).

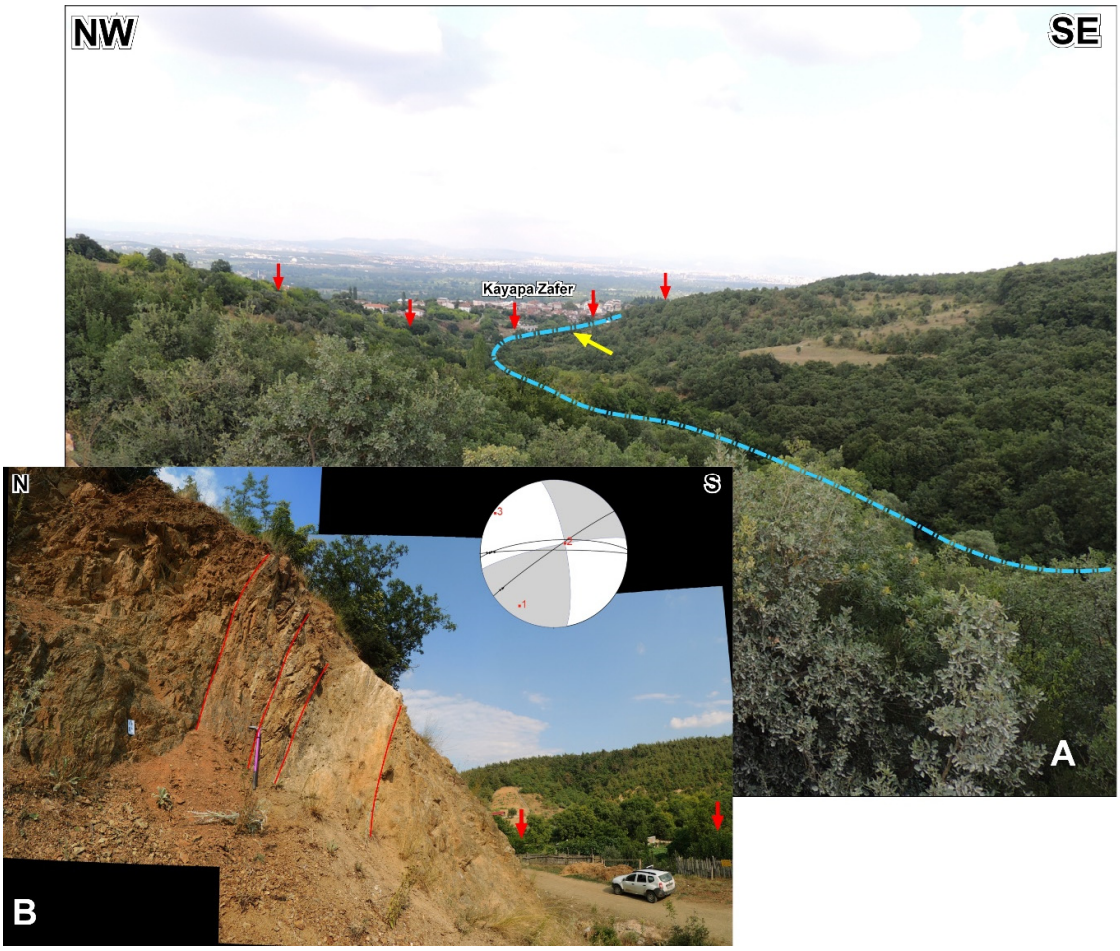

Figure A.25. A) The position of Kayapa-Yenişehir Fault (KYF) in the south of Kayapa Zafer (red arrows). Blue dashed line represents bending stream. Yellow arrow shows the location of B. **B)** A well-developed shear zone of KYF. The length of ice axe is 80 cm. The circle represents the equal area lower hemisphere spherical projection of the fault plane and slickenlines. Gray and white areas (contractional and extensional areas, respectively) are the fault plane solution obtained by kinematic analysis of the fault data. The 1, 2, and 3 indicate the orientation of kinematic (strain) axes (after Seyitoğlu et al., 2021).

Details of the Dorak-Durumtay Fault (DDF), Mustafakemalpaşa Fault (MPF), Hamamlı Fault (HMF), Ocaklı Fault (OCF), Derecik Fault (DKF), Keltaş Fault (KTF) and Karaağaç Fault (KÇF)

The southern branch of NAFZ reaches south of Ulubat Lake and it continues towards southwest with ENE-WSW and NE-SW trending right-lateral strike-slip faults of Dorak - Durumtay Fault (DDF), Mustafakemalpaşa Fault (MPF), Karacabey Fault (KBF), Susurluk - Havran Fault (SHF), and Edremit Fault (ETF) (Figure 3, 4).

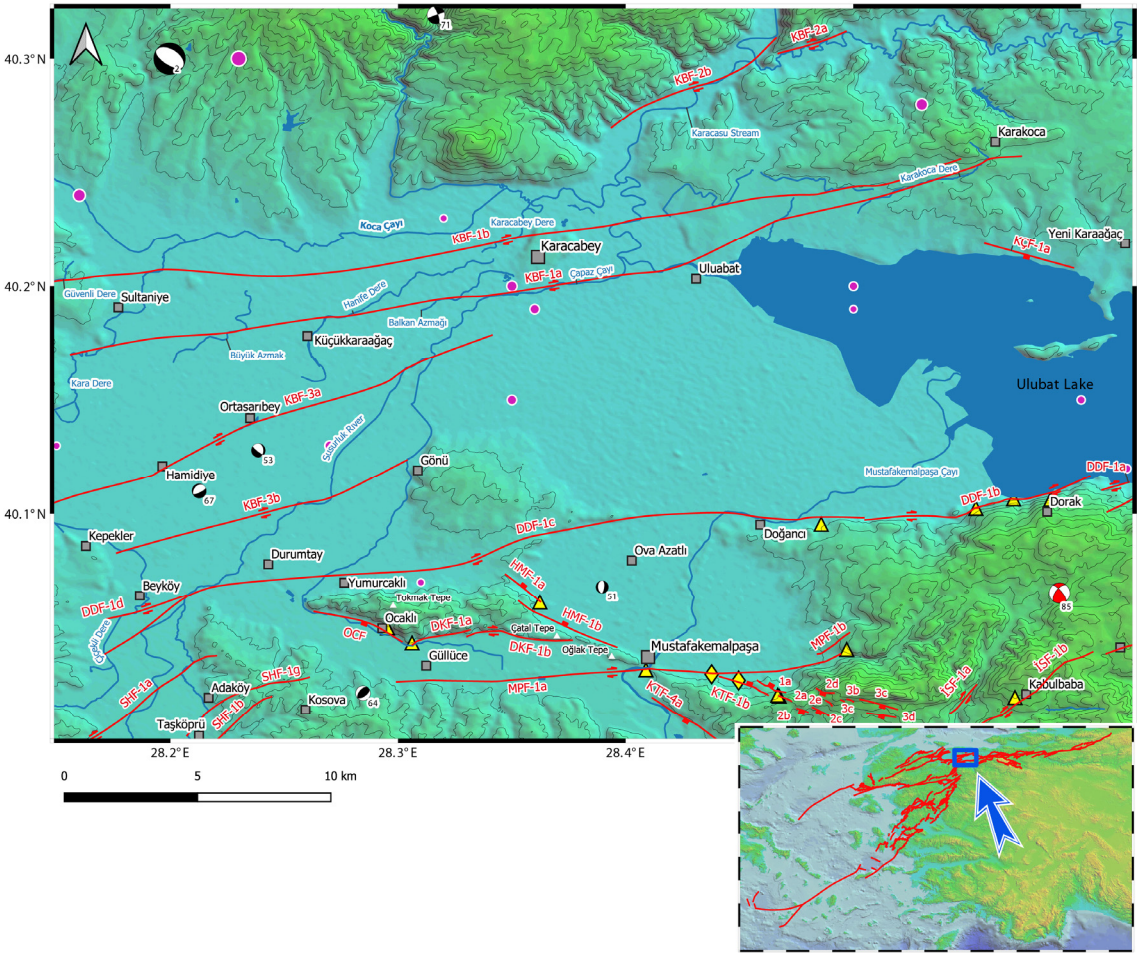

Figure A.26. The Ulubat pull-apart basin and related faults. Fuchsia dots with white circles are the epicenter locations of earthquakes (1900-2020, M≥3.5) from KOERI catalogue. For focal mechanism solutions see Appendix B. Please note distinctive multiple right lateral displacements of the stream channels along the Karacabey Fault (KBF), Dorak-Durumtay Fault (DDF), Mustafakemalpaşa Fault (MPF) and Susurluk-Havran Fault (SHF). HMF: Hamamlı Fault; OCF: Ocaklı Fault; KTF: Keltaş Fault; İSF: İnegazi-Sincansarnıç Fault. The yellow rhombic signs are paleoseismological trench locations of Kop et al. (2016). See previous studies (Emre et al., 2013; 2018 and Seyitoğlu and Esat, 2022a) for comparison.

The Dorak-Durumtay Fault (DDF) has ENE-WSW trend and traced between Dorak and Durumtay villages. The short, en echelon segment of DDF-1a are nearly parallel to the UDF. A direction changes from east-west to northeast-southwest on the segment DDF-1b in the west of Dorak creates a restraining bend in which thrust component of strike slip fault surfaces are observed (Figures A.26 and A.27).

Figure A.27. A) The bending area of DDF-1b in the south of Ulubat Lake. **B, C** and **D**) details of kinematic data (after Seyitoğlu and Esat, 2022a). The circle represents the equal area lower hemisphere spherical projection of the fault plane and slicken-lines. Gray and white areas (contractional and extensional areas, respectively) are the fault plane solution obtained by kinematic analysis of the fault data. The 1, 2, and 3 indicate the orientation of kinematic (strain) axes.

The focal mechanism solution of the seismic event #85_2015.01.23 (ML=4.5) indicates thrusting with right-lateral component, probably this solution reflects the overall change of direction on the right lateral strike-slip faulting in this area. (Figure A.26, Appendix B). Further to west, the DDF-1b and DDF-1c limit the morphological highs at the south of Ulubat Lake where a 2.6 km right-lateral displacement of the Mustafakemalpaşa Çayı measured at the north of Doğancı along the DDF-1c. This segment also creates 3.31 km right-lateral shift on the creek at the northwest of Ova Azatlı and a right bending on the stream channel in the northwest of Yumurcaklı (Figure A.26). Moreover, the DDF-1c causes 4.6 km right-lateral diversion on the (Hanife Dere) Susurluk River in the west-southwest of Durumtay. The DDF-1d creating 1.15 km right lateral shift on the Çiçekli Dere, is connected to the DDF-1c in the east

of Beyköy (Figure A.26, Appendix C). A recent seismic activity (2020.10.15; M=2.1) occur in this area but no reliable focal mechanism solution obtained.

In the west-northwest of Mustafakemalpaşa, the topographic uplift (i.e., Tokmak Tepe, Çatal Tepe, Oğlak Tepe) are bounded by the NW-SE trending Hamamlı Fault (HMF) (Figures A.26 and A.28). The NE dipping normal fault segments (HMF-1a, HMF-1b) are located on the northwest of Mustafakemalpaşa and the SW dipping Ocaklı normal fault (OCF) passes through Ocaklı village (Seyitoğlu et al., 2021; Seyitoğlu and Esat, 2022a).

The focal mechanism of the seismic event # 51_2007.06.22 (Md=2.7) seems related to the segments HMF-1a_b, although a slight rotation is needed for a perfect fit (Figure A.26; Appendices B and C).

The southern margin of Tokmak Tepe uplift is bounded by two en echelon segments of Derecik Fault (DKF-1a_b). They created 115 m and 335 m right bends on the stream channels west and east of Derecik respectively (Seyitoğlu and Esat, 2022a) (Figures A.26 and A.28).

The normal fault segments of the Karaağaç Fault (KÇF) dipping SW can be drawn on the northern side of the Ulubat Lake by using the morphology (KÇF-1a_e) (Figures A.21 and A.26).

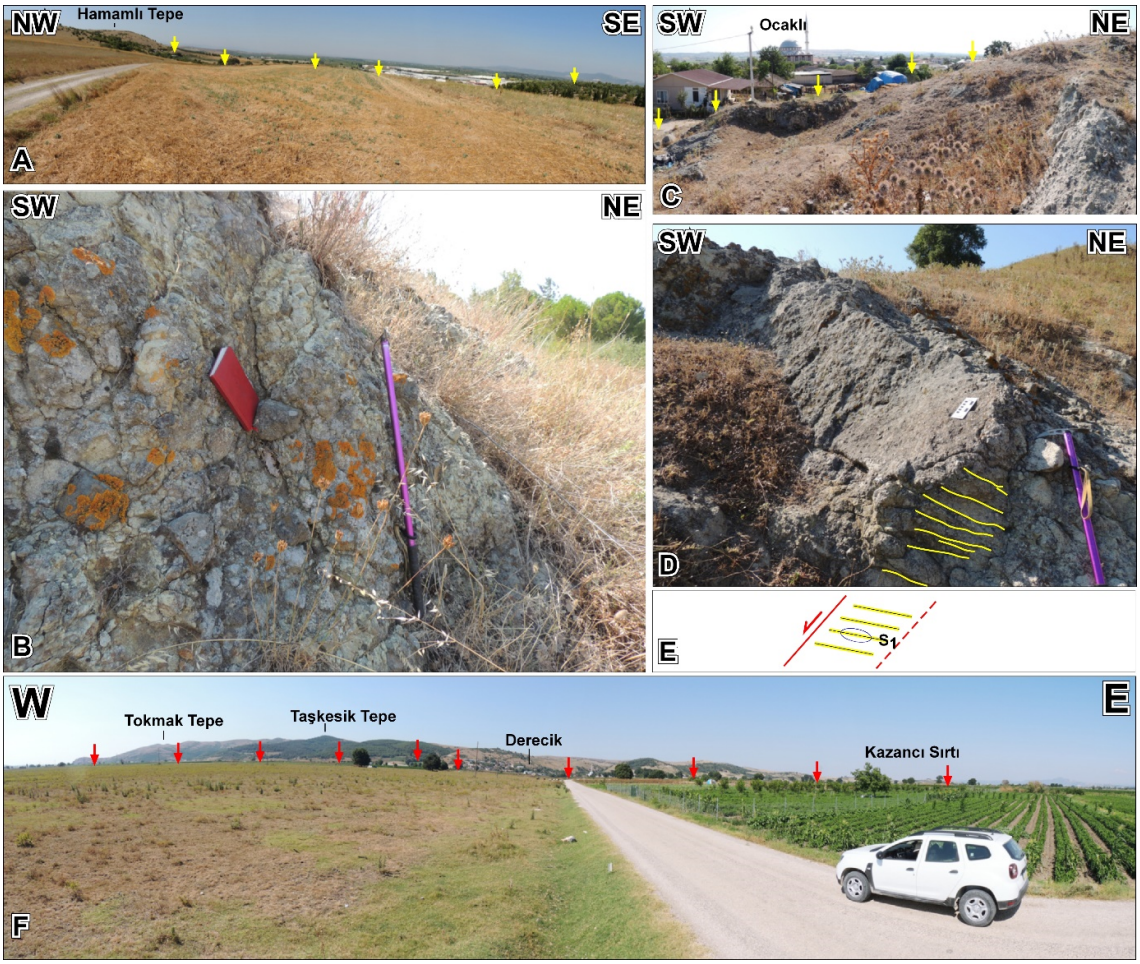

Figure A.28. A) Field view of Hamamlı normal fault. **B)** Systematic fractures parallel to the Hamamlı Fault (HMF) segments in the volcanoclastic rocks. **C)** Distinguished topographical difference along the Ocaklı normal fault in the Ocaklı settlement. **D)** Systematic fractures parallel to the OCF in the volcanoclastic rocks. **E)** Shear zone cleavage indicated normal faulting (after Seyitoğlu et al., 2021; Seyitoğlu and Esat, 2022a).

The Mustafakemalpaşa Çayı passing through the settlement bearing the same name makes a very sudden 850 m right lateral dislocation which is created by the MPF-1a of Mustafakemalpaşa Fault (MPF) continuing to west in the south of Güllüce (Figure A.26). The MPF_1a and SHF-1c of Susurluk-Havran Fault (SHF) (see below) are probably creating a restraining stepover where the focal mechanism solution of the seismic event #64_2008.10.14 (Md=3.2) indicate thrusting (Figure A.26; Appendices B and C).

The route of WSW-ENE trending of MPF-1b is quite different than that of NW-SE trending MPF of Emre et al. (2011a; 2011b). Our MPF-1a passes from the Lalaşahin trench of Kop et al. (2016) and presented kinematic data from the quarry, northeast Çördük (Fig. A.29).

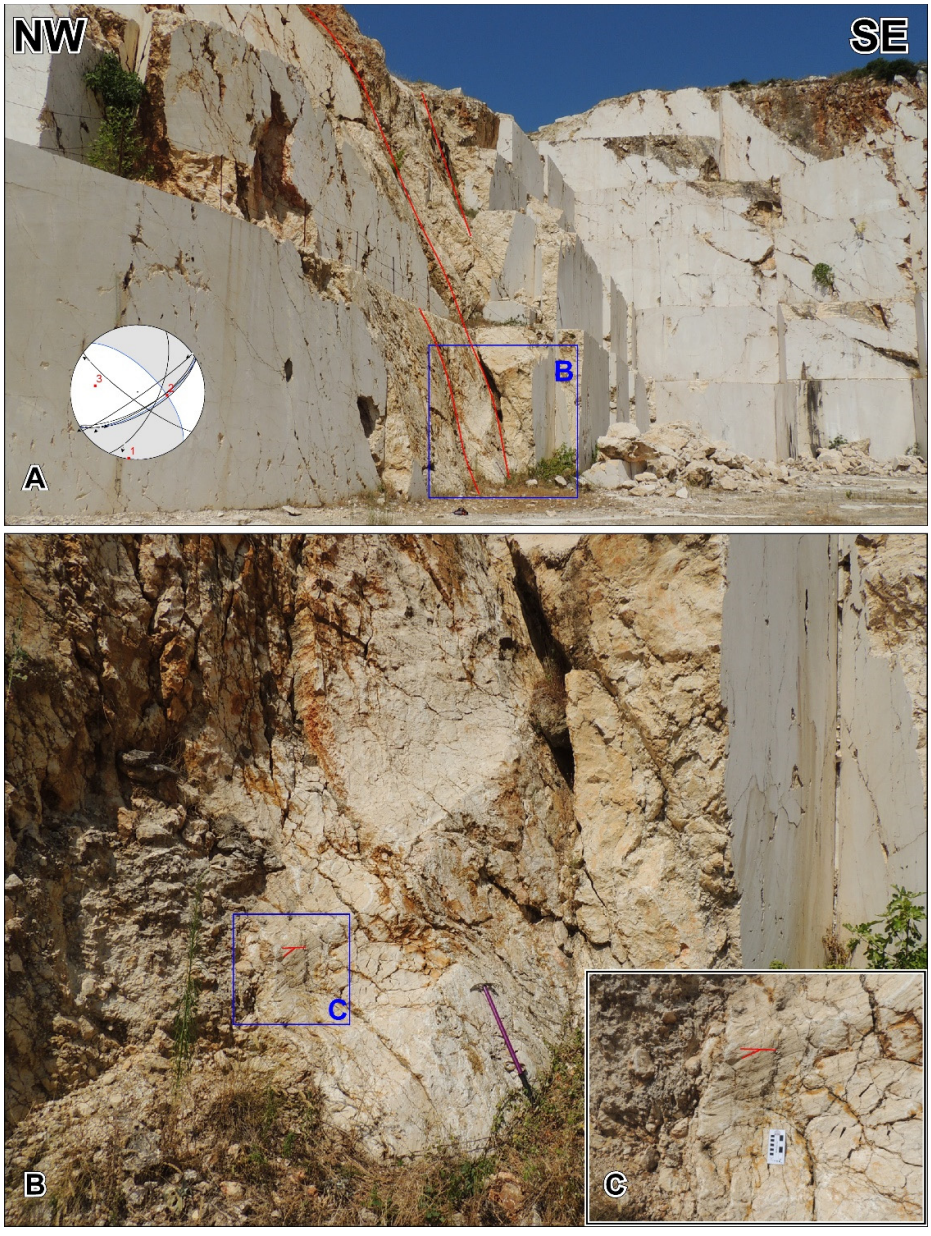

Figure A.29. A) Shear surfaces providing kinematic data at the NE end of MPF-1a in a marble quarry northeast Çördük. **B & C)** close-up views. The circle represents the equal area lower hemisphere spherical projection of the fault plane and slicken-lines. Gray and white areas (contractional and extensional areas, respectively) are the fault plane solution obtained by kinematic analysis of the fault data. The 1, 2, and 3 indicate the orientation of kinematic (strain) axes (after Seyitoğlu and Esat, 2022a).

Contrary to the southeast continuation of NW-SE trending right lateral strike-slip MPF of Emre et al. (2013), field observations (Seyitoğlu and Esat, 2022a) indicate that NW-SE trending fault segments have normal fault character dipping northeast and southwest. For this reason, they evaluated as separate structure called Keltaş Fault (KTF) which is developed in a releasing stepover between MPF and İnegazi-Sincansarnıç Fault (İSF) (Figures A.26, A.30, and A.31) (for detailed discussions see Seyitoğlu and Esat, 2022a).

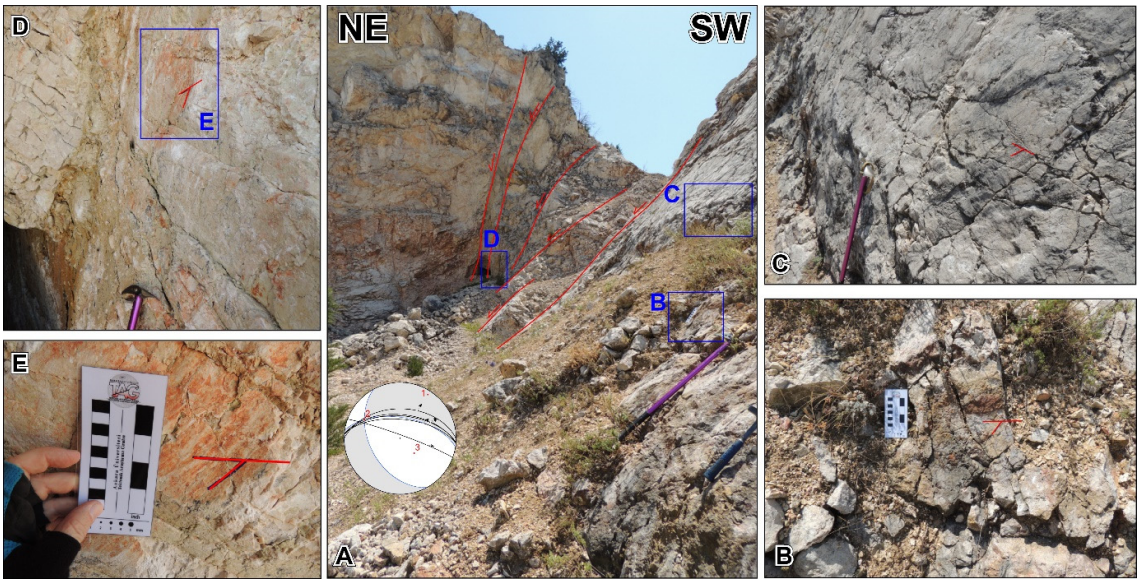

Figure A.30. A) Well-developed normal fault surfaces with right-lateral component dipping northeast in the west of Keltaş Tepe. **B_E)** Close-up views. The circle represents the equal area lower hemisphere spherical projection of the fault plane and slicken-lines. Gray and white areas (contractional and extensional areas, respectively) are the fault plane solution obtained by kinematic analysis of the fault data. The 1, 2, and 3 indicate the orientation of kinematic (strain) axes (after Seyitoğlu and Esat, 2022a).

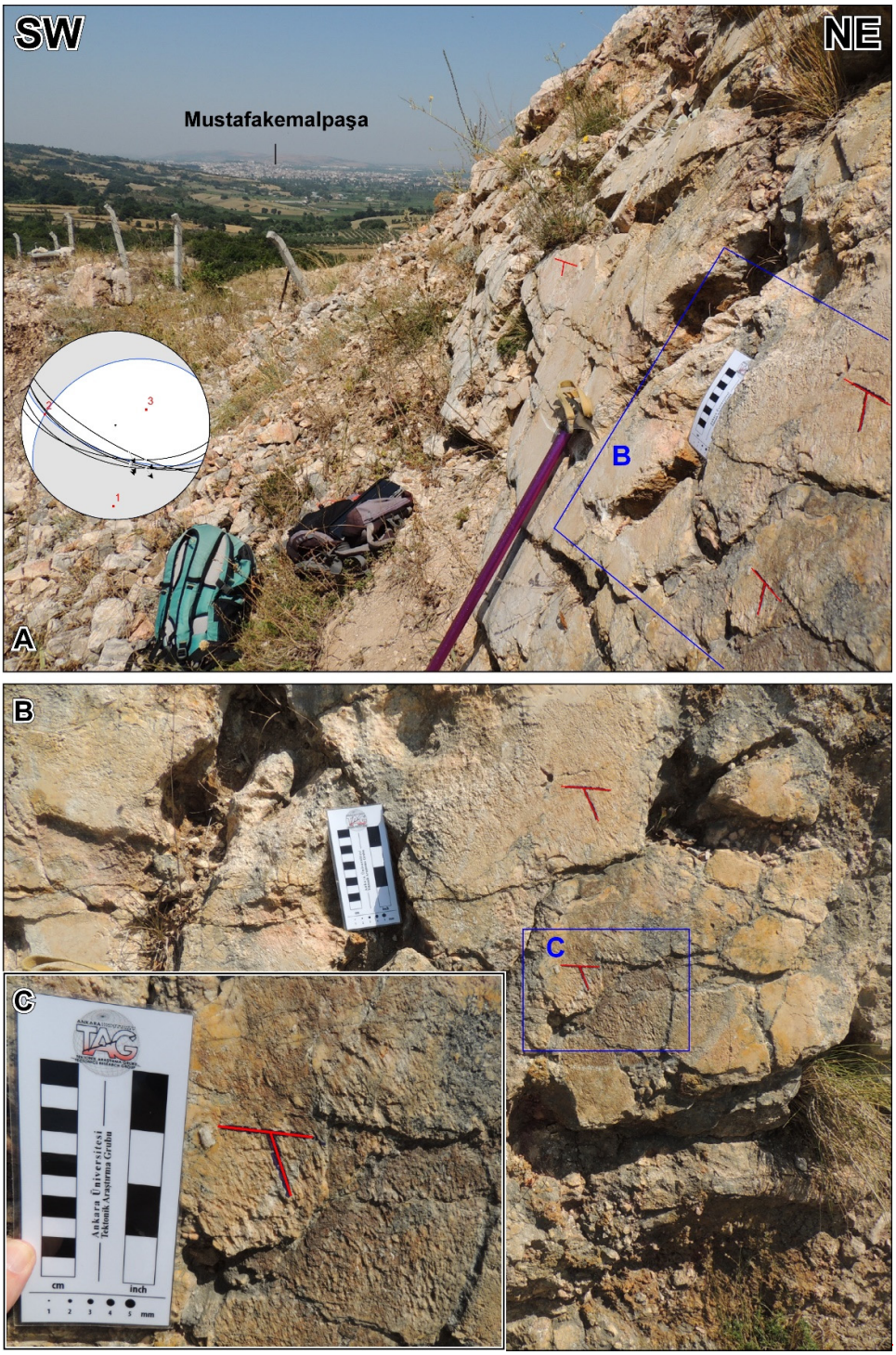

Figure A.31. A) Southwest dipping normal fault surfaces with left-lateral component of Keltaş Fault in the south of Keltaş Tepe. Photos are taken from the route of so-called Mustafakemalpaşa Fault of Emre et al. (2011a). See Seyitoğlu et al. 2021 and Seyitoğlu and Esat (2022a) for discussion. **B** and **C)** Close-up views of the fault surfaces. The circle represents the equal area lower hemisphere spherical projection of the fault plane and slicken-lines. Gray and white areas (contractional and extensional areas, respectively) are the fault plane solution obtained by kinematic analysis of the fault data. The 1, 2, and 3 indicate the orientation of kinematic (strain) axes.

Details of the İnegazi-Sincansarnıç Fault (İSF), Atlas Fault (ATF) and Doğancı Fault (DNF)

In the southwest of Kabulbaba, İnegazi-Sincansarnıç Fault (İSF) starts with en echelon NE-SW trending segments (İSF-1a_b) (Figure A.26). The segment İSF-2a is located on the spectacular, 10 km long, curvilinear Sarnıç valley at the north of Eskikızılelma. Further to northeast, two en echelon relatively short segments (İSF-2b_c) create right bending of Eskiçal Dere. Another short, en echelon, NE-SW trending segment İSF-2d is located on the Bıçkı Dere at the south of Üçpınar (Figure A.21).

In the north of Kocakoru village, curvilinear Kuzgunkaya Dere valley hosts the segment İSF-3a and extended to Korubaşı at the northeast via Sincansarnıç village. The segment İSF-3b is located on the linear valley of Alagöz Dere in Çiçekli and can be followed to the south of Kuruçeşme where an elongated ridge exists between the segments of İSF-3b and İSF-3c (Figure A.21, Appendix C) (Seyitoğlu et al., 2021).

The Atlas Fault (ATF) is composed of normal fault segments and the strike-slip transfer faults between them. The tectonic position of ATF is a releasing stepover between right-lateral strike-slip İnegazi- Sincansarnıç Fault (İSF) and Doğancı Fault (DNF). Its normal fault character has been proven by the focal mechanism solution of the seismic event #68_2009.03.08 (Md=3.1) (Figure A.21, Appendix B). The segments ATF-2a and ATF-2b are the transfer faults separating north dipping normal fault segments of ATF-3a and ATF-3b (Figure A.21, Appendix C) (Seyitoğlu et al., 2021).

The Doğancı Fault (DNF) is a right-lateral strike-slip fault as indicated by the focal mechanism solutions of the seismic events #50_2007.06.13 (Md=3.2) and #55_2007.12.03 (Md=3.2). Moreover, the structural data on the segment DNF-1a is obtained at the southwest of Doğancı (Seyitoğlu et al., 2021). DNF-1b controls the

position of Nilüfer Çayı and a 1280 m right lateral displacement is measured along this segment at the north of Doğancı. Tectonic position of Doğancı Fault is a transfer fault between opposite dipping Atlas and Gökçeören normal faults (Figure A.21; Appendices B and C) (Seyitoğlu et al., 2021).

Details of the Susurluk-Havran Fault (SHF)

In the Susurluk valley, the NE-SW trending en echelon segments constitute northeastern end of the Susurluk-Havran Fault (SHF) (Figure 4, A.32, Appendix C). The SHF-1a both forms 1.62 km right lateral displacement in the (Hanife Dere) Susurluk River and causes a 770 m right lateral offset in the route of Kara Dere at the west and north of Adaköy respectively. The southwest continuation of SHF-1a is located on the linear valley at the northwest of Yahyaköy (Figure A.32).

The northeast tip of SHF-1b is located between Adaköy and Kosova and creates 970 m right-lateral shift on the Kara Dere at the south of Taşköprü. A semi-parallel SHF-1g creates 1430 m and 265 m right lateral shifts on the course of Kara Dere between Taşköprü and Adaköy and on the Çerkez Dere at the north of Kosova respectively. Another 1.27 km right-lateral displacement is created on the (Simav Çayı) Susurluk River along the SHF-1b which also causes nearly 100 m sharp right-lateral diversion on the creek at Balıklıdere village. The overall NW-SE drainage is cut by NE-SW trending SHF-1b at the southwest of Susurluk along with linear Harap Dere (Figure A.32). The focal mechanism solution of recent seismic event #120_2020.12.11 (ML=4.1) confirm the positions of the segments SHF-1a and SHF-1b (Figure A.32, Appendix B; Seyitoğlu et al., 2020a). Near to the southwest tip of SHF 1b, spectacular fault surface, west of Ömerköy provides kinematic data indicating right lateral strike-slip faulting (Figure A.33).

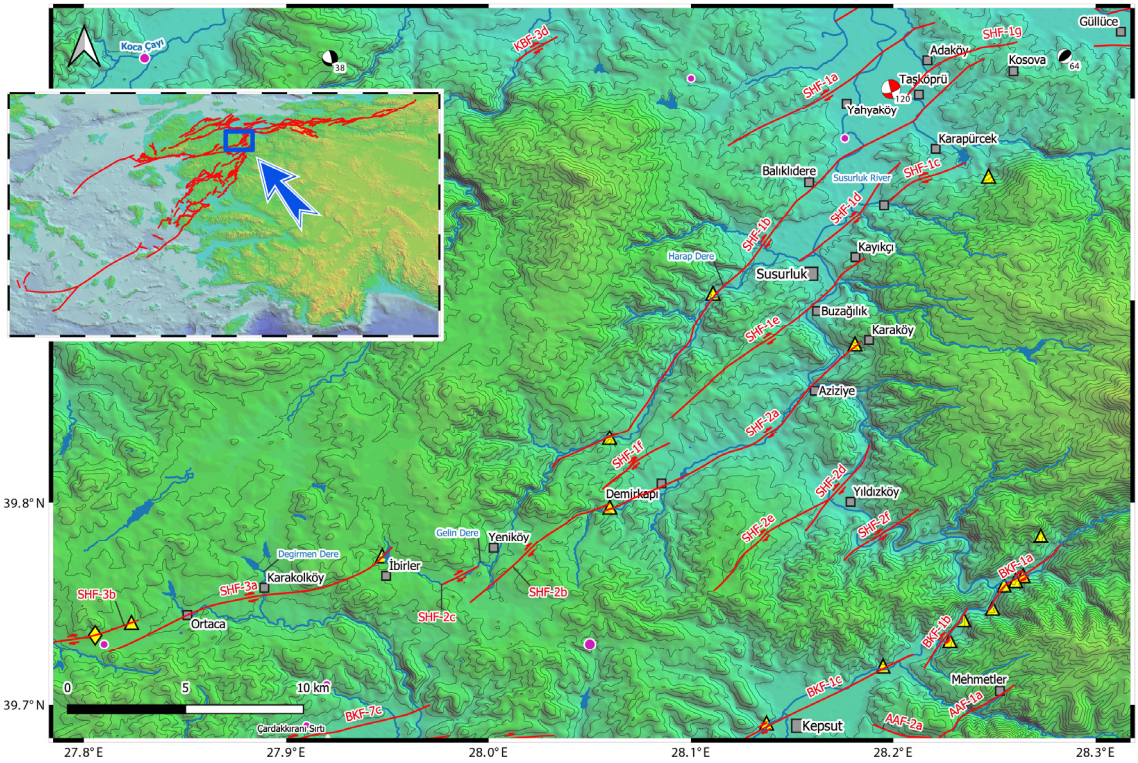

Figure A.32. The segment distribution of active faults between Susurluk and Kepsut. Please note distinctive multiple right-lateral displacements of the stream channels along the segments of Susurluk-Havran Fault (SHF) and Balıkesir-Kepsut Fault (BKF). Fuchsia dots with white circles are the epicenter locations of earthquakes (1900-2020, M≥3.5) from KOERI catalogue. For the focal mechanism solutions see Appendix B. Yellow triangles are the locations of structural data from Sümer et al. (2018) and Seyitoğlu and Esat (2022a). The yellow rhombic sign shows the location of paleoseismological trench (Sözbilir et al., 2016b). See previous studies (Emre et al., 2013; 2018; Seyitoğlu and Esat, 2022a) for comparison. AAF: Akçaköy-Ataköy Fault.

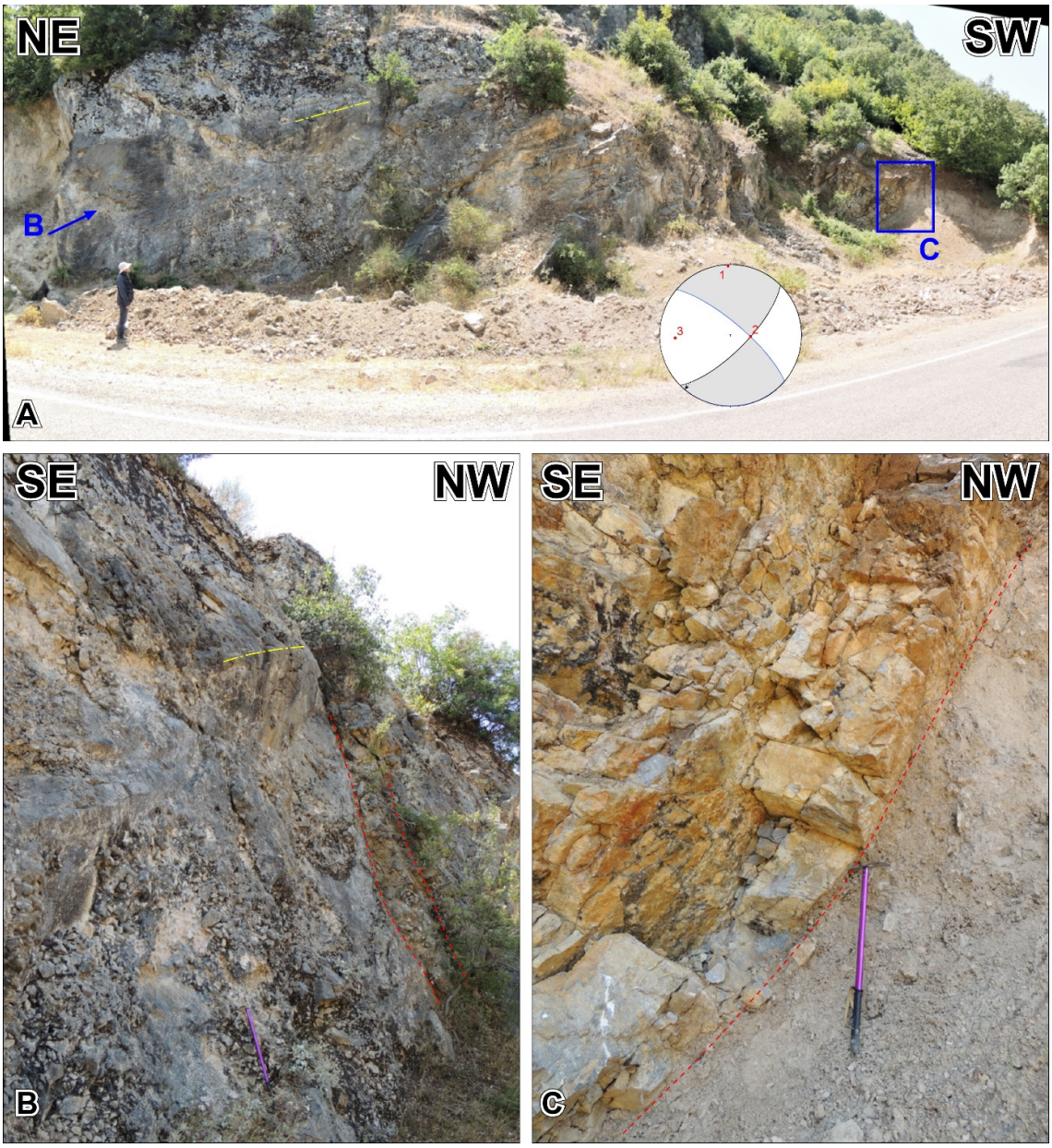

Figure A.33. A) Panoramic view of SHF-1b in the west of Ömerköy. **B)** Close up view of fault surface with the well-developed cataclastic zone. **C)** Close up view of fault surface and slope debris. The circle represents the equal area lower hemisphere spherical projection of the fault plane and slicken-lines. Gray and white areas (contractional and extensional areas, respectively) are the fault plane solution obtained by kinematic analysis of the fault data. The 1, 2, and 3 indicate the orientation of kinematic (strain) axes (after Seyitoğlu and Esat, 2022a).

The SHF-1c and -1d are located between Susurluk and Karapürçek. The SHF-1c mainly follows linear valleys between Karapürçek and Dereköy. A 2.96 km right-lateral displacement is measured on the (Simav Çayı) Susurluk River along SHF-1d, moreover bending and small scale (100 m) right-lateral shifting occurs on the

tributaries of Susurluk River. Further to south between Kayıkçı and Buzağılık, Susurluk River / Simav Çayı is displaced 2 km right-laterally by the SHF-1e. Linear valleys determine the position of en echelon SHF-1f (Figure A.32).

Similar amount of right-lateral shift (1.92 km) is also observed along the SHF-2a between Aziziye and Karaköy on the Susurluk River (Figure A.34).

Figure A.34. A) Position of SHF-2a from Karaköy to Aziziye. Note the systematic shear fractures on the Paleozoic-Triassic recrystallized limestone which is parallel to the SHF-2a. **B)** Close-up view of the shear fracture with kinematic data. The circle represents the equal area lower hemisphere spherical projection of the fault plane and slicken-lines. Gray and white areas (contractional and extensional areas, respectively) are the fault plane solution obtained by kinematic analysis of the fault data. The 1, 2, and 3 indicate the orientation of kinematic (strain) axes (after Seyitoğlu and Esat, 2022a).

The SHF-2a continue towards southwest along a linear valley between Demirkapı and Aziziye. The en echelon NE-SW trending segment SHF-2b makes a releasing offset at the southwest of Demirkapı where kinematic data are obtained inside the quarry (Figure A.35). Another right stepping short segment (SHF-2c) follows the bend of Gelin Dere at the southwest of Yeniköy. The SHF-2d_e and SHF-2f control the route of Susurluk River at the west and east of Yıldızköy, respectively (Figure A.32).

Figure A.35. A) The quarry in a releasing stepover between SHF-2a and SHF-2b, southwest Demirkapı. **B-E)** Details of fault surfaces. The circle represents the equal area lower hemisphere spherical projection of the fault plane and slicken-lines. Gray and white areas (contractional and extensional areas, respectively) are the fault plane solution obtained by kinematic analysis of the fault data. The 1, 2, and 3 indicate the orientation of kinematic (strain) axes (after Seyitoğlu and Esat, 2022a).

The SHF-3a causes sudden bends on the routes of Ortaca Dere and Gelin Dere in the east of Ortaca and in the north of İbirler respectively. In the south of Karakolköy, Değirmen Dere is shifted 580 m right-laterally along the SHF-3a (Figure A.32).

The en echelon SHF-3b makes a releasing offset with the SHF-3c which causes 530 m right-lateral shift on the Dipsiz Dere between Turplu and Deliklitaş (Figure A.32). The position of SHF-3c is somewhat correspond to the Havran-Balya Fault Zone of Emre et al. (2011a). The en echelon SHF-3d is located on the prominent linear valley where Koca Çay is 4.38 km right-laterally shifted. Small scale right-lateral displacements on the creeks located on the northwest slopes of the valley are visible. The SHF-3d is terminated in the northwest of Kocaavşar where the right bend of Kasırga Dere is obvious (Figure A.36).

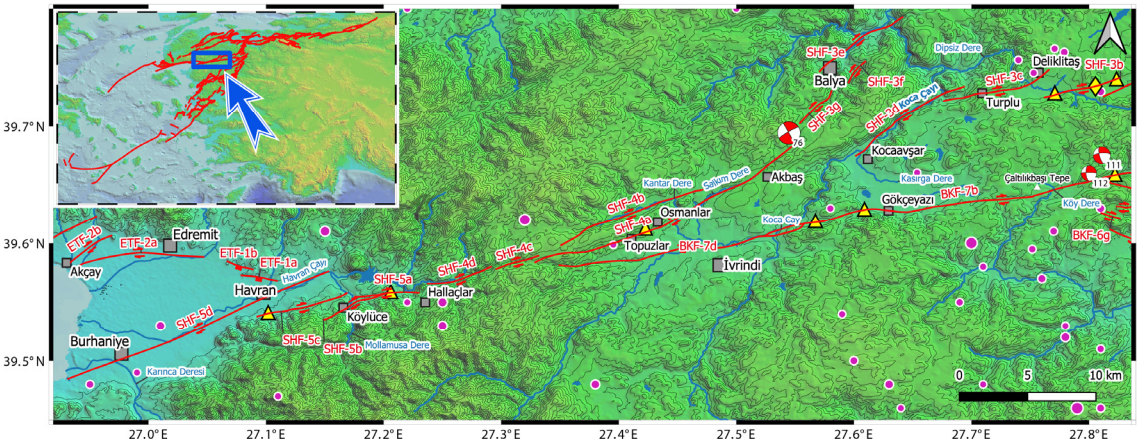

Figure A.36. The segment distribution of Susurluk-Havran Fault (SHF) and its relationship with the Edremit Fault (ETF). Fuchsia dots with white circles are the epicenter locations of earthquakes (1900-2020, M≥3.5) from KOERI catalogue. For the focal mechanism solutions see Appendix B. The yellow rhombic sign is the paleoseismological trench site of Sözbilir et al. (2016b). The yellow triangles indicate structural data locations of Sümer et al. (2018). See Emre et al. (2013; 2018) for comparison.

The right stepping SHF-4a is located on the linear valley of Salkım Dere at the west of Akbaş. It causes right bending of Kantar Dere at the east of Osmanlar where 270 m sharp displacement is measured. The SHF-4a also controls the drainage pattern at the west-soutwest of Topuzlar. The focal mechanism solution of seismic event

#76_2010.08.12 (ML=4.9) indicates NE-SW trending right-lateral strike-slip faulting that can be matched with the segment SHF-4a (Figure A.36, Appendix B). The en echelon, semi-parallel SHF-4b creates sharp bend on the Kantar Dere at the north-northeast of Osmanlar. Two right stepping relatively short segments (SHF-4c_d) reach to the north of Halaçlar where a restraining stepover is created with the SHF-5a. The arc shaped SHF-5b causes 450 m right-lateral displacement on the Mollamusa Dere in the Köylüce. The position of Havran Çayı is mainly controlled by the SHF-5d and creates distinctive bends on the Havran Çayı at northeast Burhaniye and Karınca Deresi in Burhaniye (Figure A.36, Appendix C).

Details of the Edremit Fault (ETF)

The Edremit Fault (ETF) is located on the northern margin of Edremit Gulf between Havran and Behram (Figure 4). In the north of Havran, the en echelon segments (ETF-1a_b) are WNW-ESE trending, SW dipping normal faults. They developed in the releasing offset between Susurluk-Havran Fault and Edremit Fault where the Edremit Plain is located (Figure 4, A.36).

The ETF is composed of NE-SW right-lateral strike-slip fault segments (ETF-2b_g; ETF-4a) and in the releasing offsets, there are WNW-ESE trending normal faults (ETF-3a_d) between Akçay and Altınoluk (Figure A.37). In the west of Altınoluk, the right-lateral strike-slip segments have a ENE-WSW trend (ETF-4a_i; ETF-5a_f; ETF-6a_g; EFT-7a_d; EFT-8a_c; ETF-9a_c) (Figure A.37, A.38, and Appendix C).

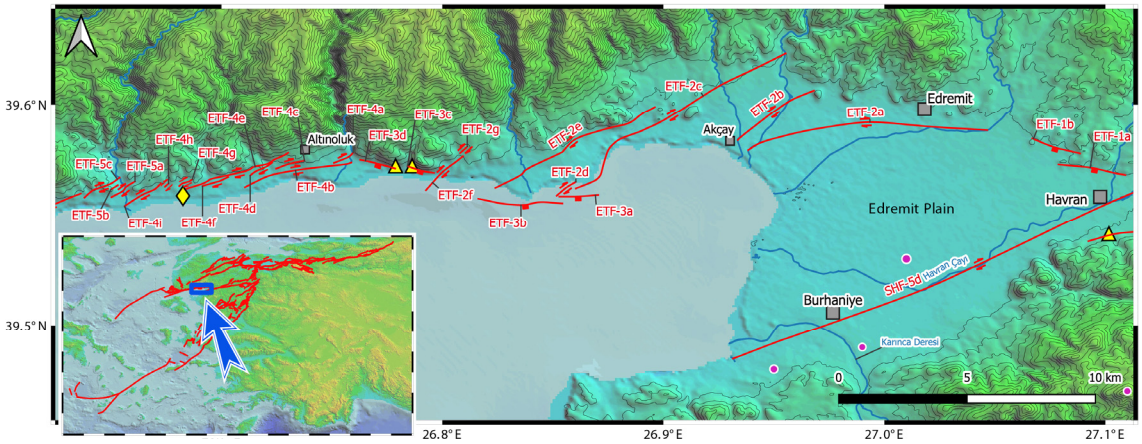

Figure A.37. The segments of Edremit Fault (ETF) between Edremit and Altınoluk. Fuchsia dots with white circles are the epicenter locations of earthquakes (1900-2020, M≥3.5) from KOERI catalogue. The yellow rhombic sign is the location of paleoseismological trench from Sözbilir et al. (2016a). The yellow triangles are the locations of surface deformations observed by Sözbilir et al. (2016a) at necropolis and terrace houses of Antandros (see discussion for details). See previous studies (Emre et al., 2013; 2018; Sözbilir et al., 2016a; Gürer et al., 2016) for comparison. SHF: Susurluk-Havran Fault.

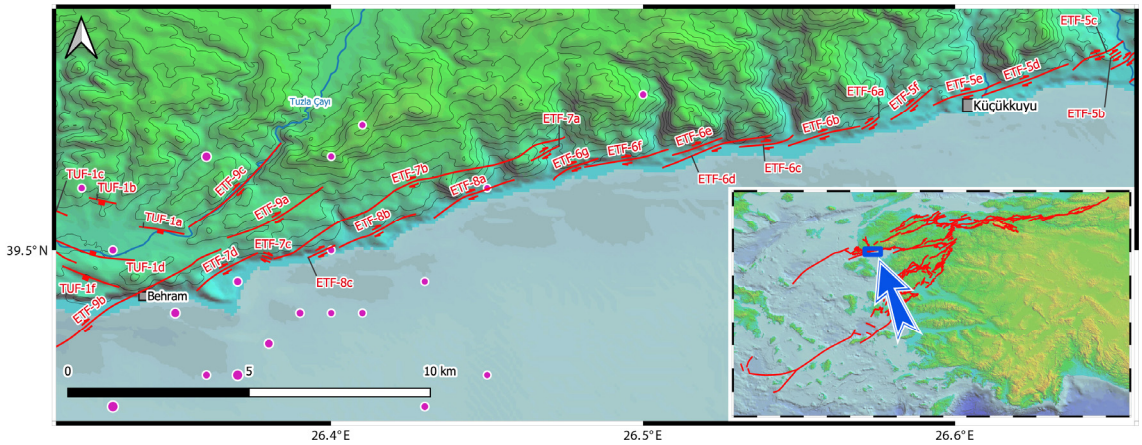

Figure A.38. The segments of Edremit Fault (ETF) between Küçükkuyu and Behram. Fuchsia dots with white circles are the epicenter locations of earthquakes (1900-2020, M≥3.5) from KOERI catalogue. See previous studies (Emre et al., 2013; 2018; Sözbilir et al., 2016a; Gürer et al., 2016) for comparison. TUF: Tuzla Fault.

Details of the Karacabey Fault (KBF)

Overall role of KBF is to separate Ulubat and Manyas lakes (Figure A.21, A.26, and Appendix C). The ENE-WSW trending KBF-1a creates several right-lateral displacements on the stream channels. These are from the northeast to southwest; (1) a 4.73 km on Karakoca Dere at the southwest of Karakoca, (2) a 220 m on a creek at the southwest of Kangal Farm, (3) a 5.15 km on Çapaz Çayı at the south of

Karacabey (Seyitoğlu *et al*., 2016), (4) a 950 m on Balkan Azmağı at the southwest of Karacabey, (5) a 700 m on Hanife Dere at the northeast of Küçükkaraağaç, (6) a 700 m on Büyük Azmak at the northwest of Küçükkaraağaç, (7) a 1.62 km on the Kara Dere at the south-southwest of Sultaniye (Figure A.26).

Further to north, the en echelon segment KBF-1b follows elongated ridges and displacements of the streams. This segment creates 1.12 km right-lateral diversion on the Koca Dere at the northeast of Karacabey. There are systematic right-lateral shifts on the stream channels at the west of Karacabey along the KBF-1b such as, a 950 m displacement on the Karacabey Dere, an 820 m shift on Kara Dere at northeast of Sultaniye, a 487 m displacement on Güvenli Dere at the northwest of Sultaniye (Figure A.26). The KBF-2a and KBF-2b correspond partly to the Karacabey Fault of Emre et al. (2011b). The Karacasu stream is right-laterally shifted approximately 6 km along the KBF-2b (Figure A.26).

The KBF-3a is another segment identified by successive river bends and displacements in the Karacabey Plain. This segment starts from the south of Karacabey and creates 1.29 km of right-lateral displacement on the (Hanife Dere / Canbalı Dere) Susurluk River towards southwest. The displacement (1.02 km) in the abandoned stream channel in the south of Ortasarıbey, the displacement (360 m) in the south of Hamidiye, and direction change of the stream channel at the northeast of Ilıcaboğazı all are the morphological elements showing the position of the KBF-3a (Figure A.26). The segment KBF-3a also clearly, right-laterally shifts the Mürvetler Dere (800 m) at the northwest of Ilıcaboğazı village (Figure A.39). Other semi-parallel KBF-3b, which is determined by bending of stream channels and 1.23 km right-lateral displacement of the (Hanife Dere) Susurluk River, is located between Gönü and

Kepekler. Its en echelon segments (KBF-3c_d) are located on the east of Manyas which are mainly control the route of Mürvetler Dere (Figure A.39).

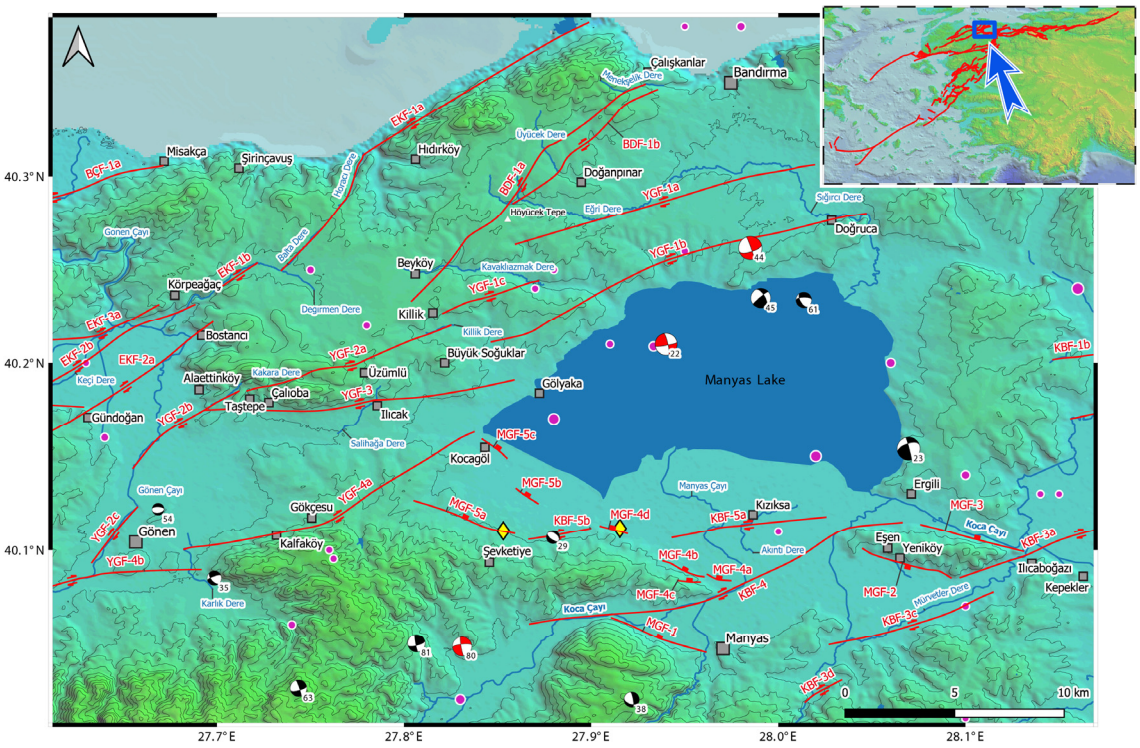

Figure A.39. The active faults between Bandırma, Gönen and Manyas. Fuchsia dots with white circles are the epicenter locations of earthquakes (1900-2020, M≥3.5) from KOERI catalogue. For the focal mechanism solutions see Appendix B. The yellow rhombic signs are the locations of paleoseismological trench sites of Kürçer et al., (2017). See previous studies (Herece, 1990; Emre et al., 2013; 2018; Kürçer et al., 2019) for comparison. BÇF: Biga-Çan Fault; BDF: Bandırma Fault; EKF: Edincik Fault; YGF: Yenice-Gönen Fault; MGF: Manyas Gölü Fault; KBF: Karacabey Fault.

The KBF-4 is defined by using 8.40 km right-lateral offset on the Manyas Çayı (Koca Çay) (Seyitoğlu et al., 2016) and its northeastern continuation also creates 938 m right-lateral diversion on the branch of Kara Dere at the northwest of Eşen. This segment is responsible for the seismic events #80_2011.03.30 (ML=4.3) and #81_2011.03.30 (Md=3.9) having strike-slip focal mechanism solutions (Figure A.39, Appendix B). The en echelon ENE-WSW trending segments of KBF-5a and KBF-5b are located between north of Şevketiye and west of Ergili at the southern Lake Manyas (Figure A.39). While the KBF-5a produces right-lateral shifting on the Manyas Çay (740 m) and on the Akıntı Dere (415 m) at the Kızıksa (Kızılköy), the KBF-5b causes right-lateral bending

in small creeks. Especially the morphological data along the KBF-5a is quite strong demonstrating the strike-slip nature of Karacabey Fault. This argument is also supported by the focal mechanism solution of the seismic event #23_2003.06.09 (Md=5.1) (Figure A.39, Appendix B).

Details of the Manyas Gölü Fault (MGF)

The NE dipping normal fault (MGF-1) limits the plain in the west of Manyas. The WNW-ESE trending, NE and SW dipping normal faults (MGF-2 and MGF-3) (i.e., Kürçer et al., 2017) form a horst where Eşen and Yeniköy are located (Figure A.39). These normal faults (MGF-1, MGF-2, MGF-3) can be interpreted as the releasing offset structures between the strike-slip faults of KBF-4 and KBF-3a_c. Similar interpretation is also plausible for the normal fault segments (MGF-4a_d and MGF-5a_c) at the south of Manyas Lake. The focal mechanism solution of the seismic event #29_2005.05.06 (Md=3.0) may be related to the segment MGF-5a, although a slight northwesterly shifting of the epicenter is needed (Figure A.39; Appendices B and C).

Details of the Yenice-Gönen Fault (YGF)

YGF-1a is determined by the right-lateral displacement (2.5 km) on Eğri Dere at the south of Doğanpınar and can be extended to the south of Bandırma. The semi-parallel YGF-1b is responsible for the sharp bending of Sığırcı Dere in Doğruca (Figure A.39). It also creates 1000 m right-lateral displacement on the tributary of Sığırcı Dere at the west of Doğruca and reaches to the northeast of Büyüksoğuklar by bending of stream channels. The focal mechanism solutions of the seismic events #44_2006.10.20 (ML=5.2) and #45_2006.10.20 (Md=4.4) confirm the right-lateral strike-slip nature of YGF-1b (Figure A.39; Appendices B and C).

The segment YGF-1c is recognized by a series of springs at the east-northeast of Killik, and also causes the shift on the route of Kavaklıazmak Dere (Figure A.39). The NE-SW trending linear Killik Dere defines the position of YGF-2a which also follows linear valleys at the north of Üzümlü and Çalıoba. The YGF turns to the direction of NNE-SSW with the segment YGF-2b following linear valley of Kakara Dere between Taştepe and Alaettin (Figure A.39). The Gönen Çayı is right-laterally displaced (2300 m) along the YGF-2b. The en echelon YGF-2c controls the position of Gönen Çayı by creating right-lateral displacement. Its position nearly parallel to the surface rupture of 1953.03.18 (M=7.2) earthquake (Emre et al., 2011b) in the Gönen city centre (Figure A.39).

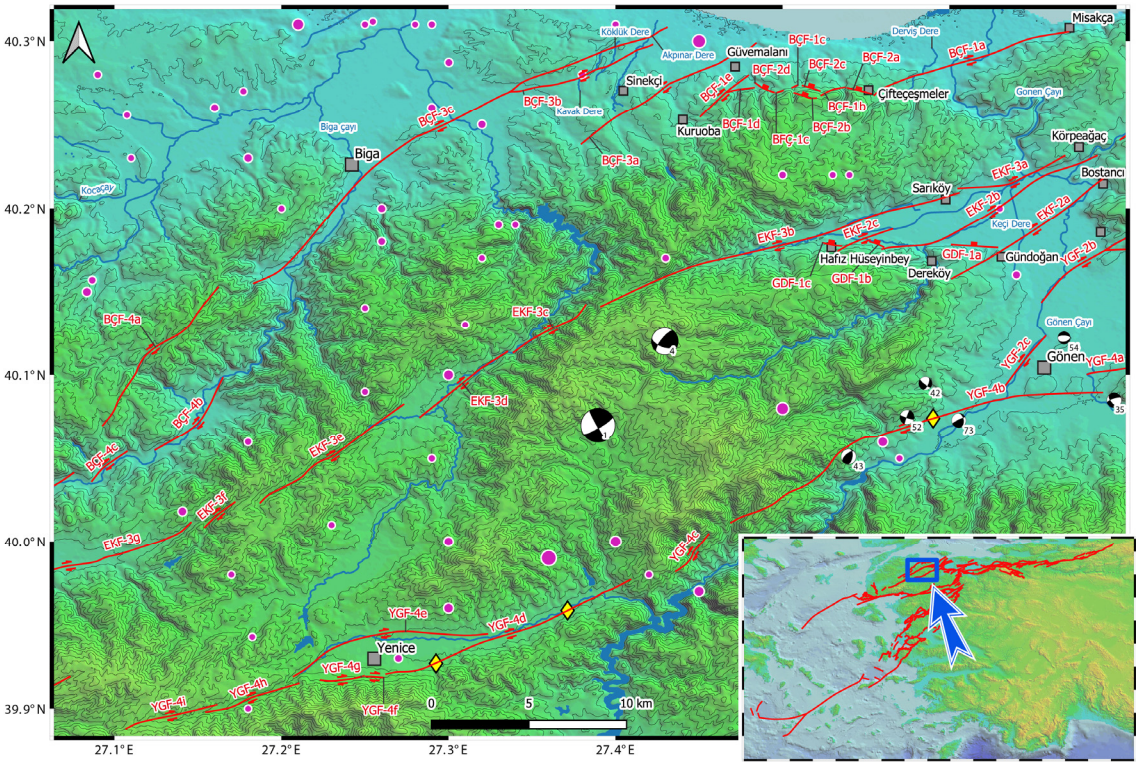

Figure A.40. The active faults between Biga, Yenice and Gönen. Fuchsia dots with white circles are the epicenter locations of earthquakes (1900-2020, M≥3.5) from KOERI catalogue. For the focal mechanism solutions see Appendix B. The yellow rhombic signs are the paleoseismological trench sites from Kürçer et al. (2008; 2019). See previous studies (Herece, 1990; Emre et al., 2013; 2018) for comparison. BÇF: Biga-Çan Fault; EKF: Edincik Fault; YGF: Yenice-Gönen Fault; GDF: Gündoğan Fault.

The ENE-WSW trending YGF-3 is defined by bending streams between north of Gölyaka and Ilıcak where 140 m right-lateral displacement is measured on the Salihağa Dere. The YGF-3 is connected to the segment YGF-2b at the south of Alaettin (Figure A.39).

The YGF-4a can be traced between Kocagöl and Gökçesu by the displacements and bends of the streams. The YGF-4a also corresponds to the surface ruptures of 1953.03.18 (M=7.2) earthquake (Emre et al., 2011b) between Gökçesu and Kalfaköy. The segment reaches to east of Gönen where a 370 m sharp right-lateral displacement is created on the Karlık Dere (Figure A.39). The YGF-4b causes an 850 m right-lateral shift on the Gönen Çay and continues towards southwest as Yenice-Gönen Fault of Emre et al. (2011b) which is drawn by following surface rupture of the #1_1953.03.18 (M=7.2) earthquake (YGF-4b_i). The seismic activity is continuing especially along the segment YGF-4b (Figure A.40, Appendix B).

Details of the Bandırma Fault (BDF)

The segment BDF-1a is located in the linear Menekşelik Dere valley at the south of Çalışkanlar and creates right bending of Üyücek (Ağa) Dere and Eğri Dere and passes to the west of elongated Höyücek Tepe and controls the position of Kavaklıazmak Dere in Beyköy. The semi-parallel BDF-1b joins to the BDF-1a at Höyücek Tepe (Figure A.39, Appendix C).

Details of the Edincik Fault (EDF) and Gündoğan Fault (GDF)

In the southwest of Erdek, the Edincik Fault of Emre et al. (2011b) was drawn on the isthmus between Kapıdağ peninsula and Bandırma (Figure 4). The best candidate for the southwest continuation of Edincik Fault (EKF) is the linear Horacı Dere valley between Şirinçavuş and Hıdırköy which is marked by EKF-1a. Its southwest

continuation is located linear Balta Dere (Figure A.39, Appendix C). The en echelon EKF-1b follows the NE-SW trending part of arc shaped Değirmen Dere. There are two NE-SW trending parallel segments which crosscut the northern Gönen Plain affecting the position of Gönen Çayı. The EKF-2a lies between west of Gündoğan and Bostancı and a 1950 m right-lateral shifting is measured at the southwest of Bostancı where the Gönen Çayı has a nearly 90^{o} sharp bend (Figure A.39). Moreover, a stream channel is 350 m right-laterally displaced at the west of Gündoğan along the EKF-2a. The EKF-2b creates distinguished right-lateral diversion (4400 m) on the route of Keçi Dere at the north of Dereköy in the northern Gönen Plain. The en echelon EKF-2c is located at the east of Hafız Hüseyinbey (Figure A.40). The EKF-3a is located between the south of Körpeağaç and Sarıköy and a 1000 m right-lateral shift is measured on Keçi Dere. In the northeast of Sarıköy, an elliptical hill is interpreted as a pressure ridge (Figure A.40). Therefore, the segment EKF-3b starts at the south of this hill and continues towards southwest. The segments (EKF-3b_g) somewhat correspond to the Sarıköy Fault of Emre et al. (2011b) (Figure A.40).

The NE-SW trending en echelon right lateral segments of Edincik Fault (EKF) (i.e., EKF-2a_c; EKF-3b) are responsible for the development of nearly WNW-ESE trending, NE dipping normal fault segments (GDF-1a_c) of Gündoğan Fault (GDF) (Figure A.40, Appendix C).

Details of the Biga-Çan Fault (BÇF)

We do not agree with the evaluation of Sinekçi Fault of Emre *et al*. (2011b) and it would be better to put together the structures in this area under the title of Biga-Çan Fault (BÇF). The overall structure between Misakça and Kuruoba is composed of the NE-SW trending right-lateral strike-slip segments and NW-SE trending, NE dipping

normal faults (Figure A.40). This approach is different than the Sinekçi Fault which was previously mapped as three segments and a thrust component marked on the middle segment (Emre et al., 2011b).

The BÇF-1a lies between Misakça and Çifteçeşme villages and creates a right-lateral displacement of 2.15 km on Gönen Çayı and 500 m on Derviş Dere (Figure A.40, Appendix C). The en echelon short segments (BÇF-1b_e) reach northeast of Kuruoba. WNW-ESE trending, NE dipping en echelon normal fault segments are located on the mountain - piedmont junction (BÇF-2a_d) (Figure A.40). The right-lateral displacements measured in the creeks along the BÇF-3a are ranging from 200 m to 82 m (Figure A.40). The displacements measured on the creeks along the BÇF-3b are 153 m on an unnamed creek, 60 m on Akpınar Dere, 530 m on Köklük Dere and reach to the 1.11 km on Kavak Dere at the northwest of Sinekçi. The BÇF-3c is responsible for the important right-lateral dislocations on the streams. These dislocations from the northeast to southwest are 445 m on an unnamed stream, 300 m on Akpınar Dere, 700 m on Kavak Dere and 7.4 km on the Biga Çayı near the Biga settlement. (Figure A.40). The segments (BÇF-4a_e) are equivalent of Biga-Çan Fault Zone of Emre et al. (2011b), but our segment distributions are different. The seismic event #98_2018.05.03 (ML=4.5) indicate that this zone is active (Figures 4, A.40, and A.41).

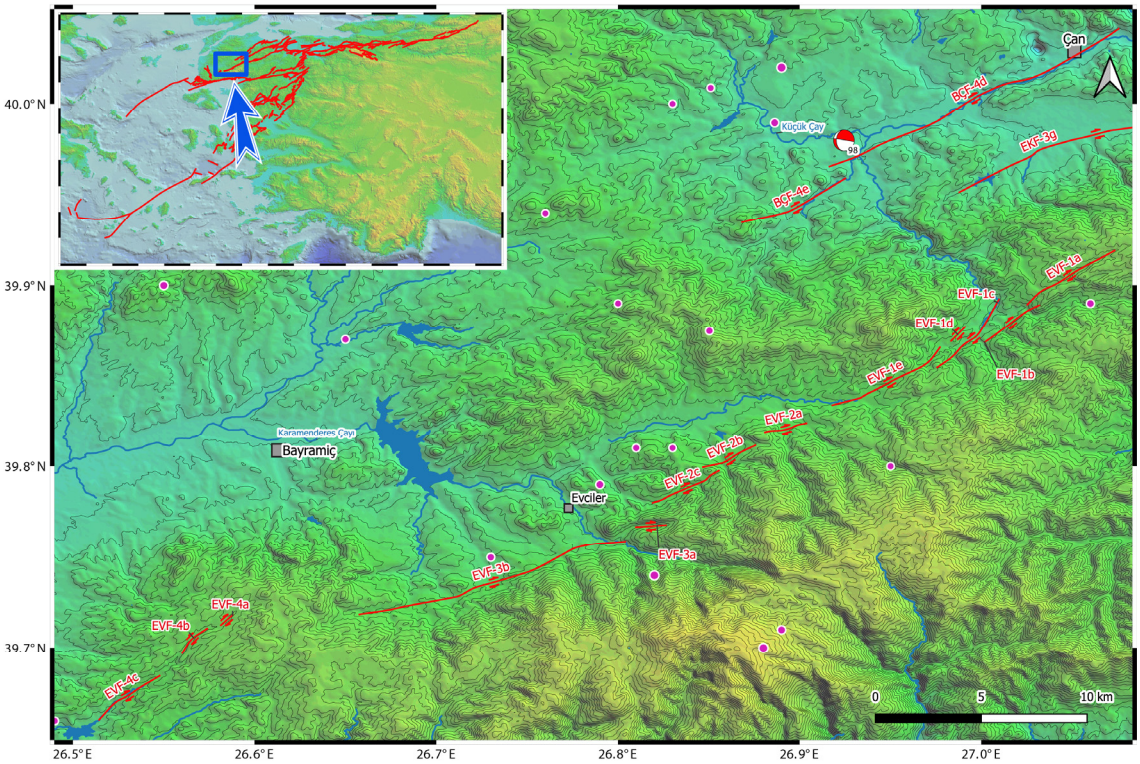

Figure A.41. The segment distribution of Evciler Fault (EVF) and southwest end of Biga-Çan Fault (BÇF). Fuchsia dots with white circles are the epicenter locations of earthquakes (1900-2020, M≥3.5) from KOERI catalogue. For the focal mechanism solutions see Appendix B. See previous studies (Emre et al., 2013; 2018) for comparison.

Details of the Evciler Fault (EVF), Ayvacık-Ezine Fault (AEF), Tuzla Fault (TUF), Babakale Fault (BAF) and İskiri-Biga Fault (İBF)

Although the segment definitions are slightly different and additional unrecognized segments at the southwestern end, the segments the Evciler Fault (EVF) are somewhat corresponding to the Emre *et al*. (2011a) (Figure A.41).

The Ayvacık-Ezine Fault (AEF) is composed of a series of NW-SE trending normal fault segments, dipping NE and constitute the northern margin of Yivlidağ horst (AEF-1a_b; AEF-2a_d; AEF-3a_b; AEF-4a_f; AEF-5a_b) (Figures 4, A.42, and Appendix C).

The southern margin of Yivlidağ horst is controlled by the normal faults creating three steps in topography (Figure 4). The first is the Tuzla Fault (TUF) contains generally

NW-SE trending normal faults, dipping SW (TUF-1a_c; TUF-1f_h; TUF-3c; TUF-5c_d; TUF-7a_d) (Figure A.43). On the other hand, antithetic faults dipping N, NW and NE are recognized (TUF-1d_e; TUF-3a_b; TUF-5a_b; TUF-8a_d). These normal faults are separated by the short NE-SW trending transfer faults. (TUF-2; TUF-4; TUF-6). The Tuzla normal fault is active and responsible for the seismic events #89_2017.02.06 (Mw=5.4), #90_2017.02.06 (Mw=5.2), #91_2017.02.07 (Mw=5.4) (Figure A.43; Appendices B and C).

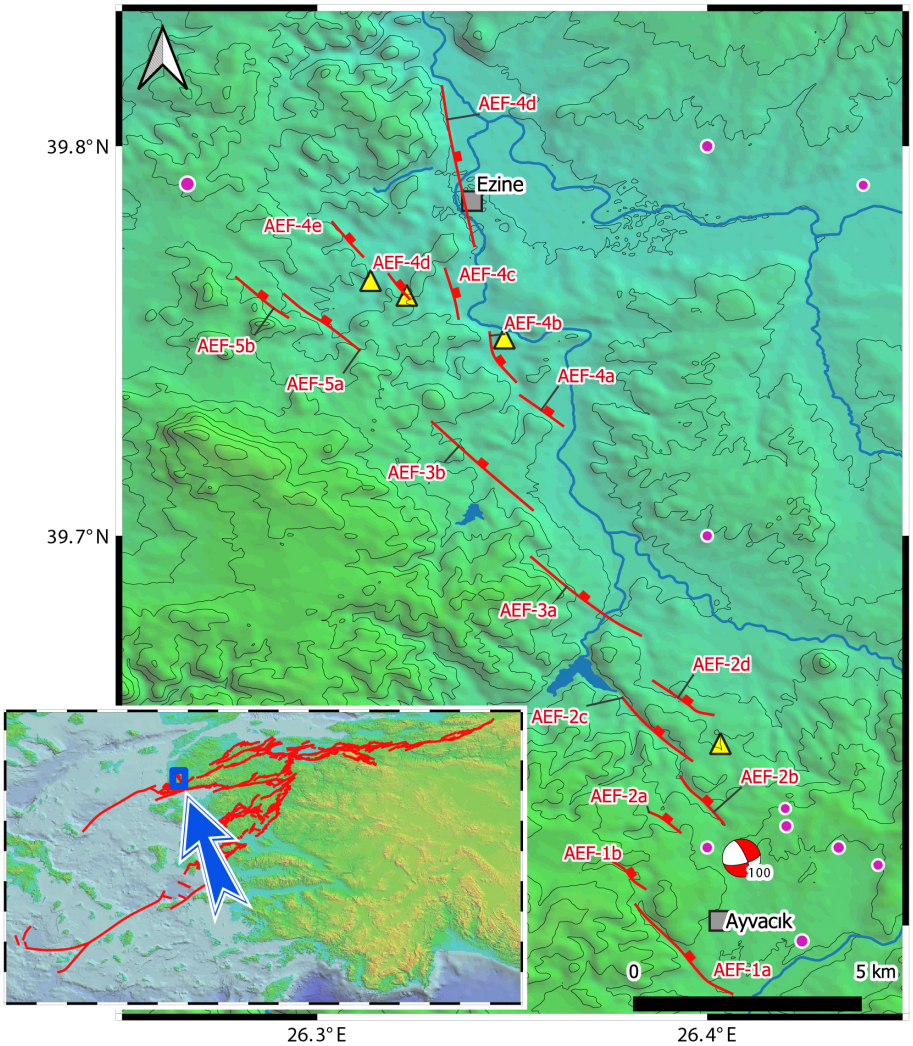

Figure A.42. The segment details of Ayvacık-Ezine Fault (AEF). Fuchsia dots with white circles are the epicenter locations of earthquakes (1900-2020, M≥3.5) from KOERI catalogue. For the focal mechanism solutions see Appendix B. Yellow triangles are selected structural data from Gürer et al. (2021).

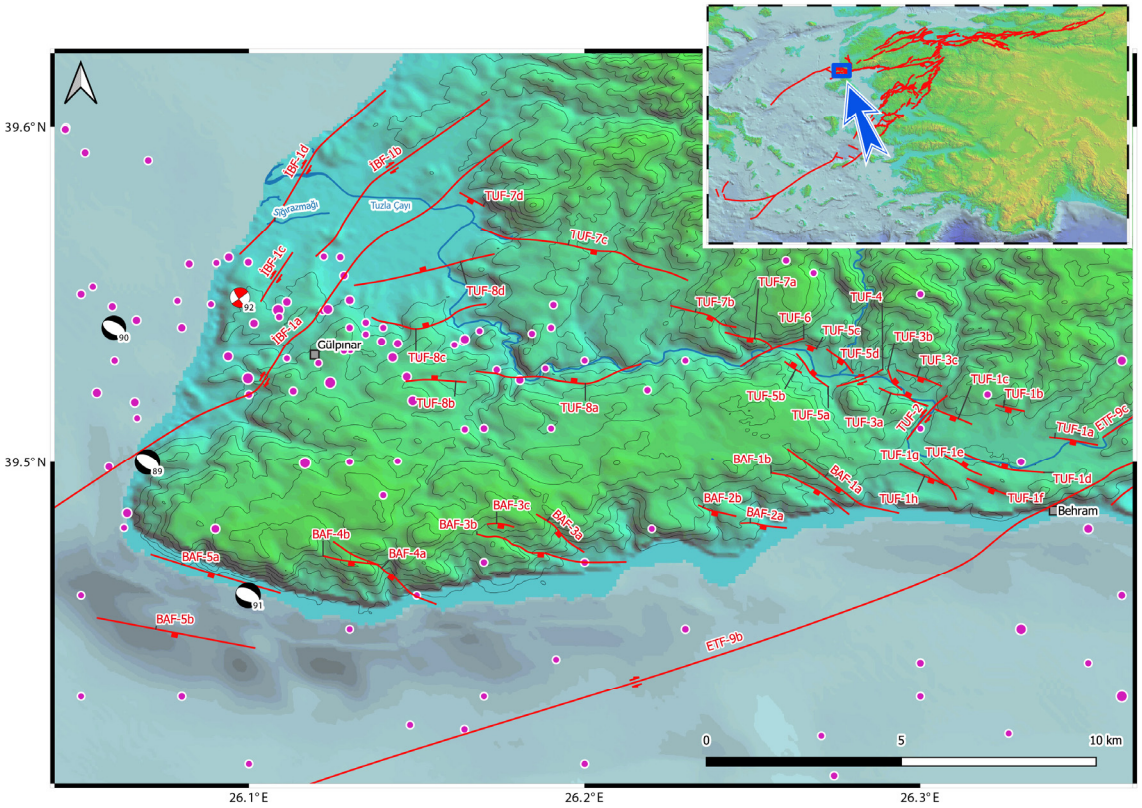

Figure A.43. The active faults around Bababurnu, southwest end of Biga peninsula. Fuchsia dots with white circles are the epicenter locations of earthquakes (1900-2020, M≥3.5) from KOERI catalogue. For the focal mechanism solutions see Appendix B. See previous studies (Yaltırak et al., 2012; Emre et al., 2013; 2018) for comparison. İBF: İskiri-Biga Fault; TUF: Tuzla Fault; BAF: Babakale Fault, ETF: Edremit Fault.

The second step of the southern margin of Yivlidağ horst is the Babakale Fault (BAF) (Figure 4) which has NW-SE trending, SW dipping several short normal fault segments (BAF-1a_b; BAF-2a_b; BAF-3a_b; BAF-4a_b). The third step (BAF-5a_d) is documented by Yaltırak et al. (2012) by using bathymetry and seismic reflection data under the Aegean Sea (Figure A.43, Appendix C). The overall structure of southwest edge of Biga Peninsula is a releasing offset (Yivlidağ horst and a pull-apart basin at Bababurnu in the Aegean Sea, Yaltırak et al., 2012) between the Edremit Fault (ETF) and İskiri-Biga Fault (İBF) (Seyitoğlu et al., 2017) (Figure 4). The segment of İskiri-Biga Fault (İBF-2) is defined by using seismic reflection and bathymetry data from Yaltırak et al. (2012) under the Aegean Sea. Its strike-slip character is confirmed by the seismic event #104_2019.10.10 (ML=4.5) (Figure A.44). Moreover, some of the

segments of right-lateral strike-slip İBF can be followed at Gülpınar which are approved by the focal mechanism solution of the seismic event #92_2017.03.24 (ML=4.3). They (İBF-1a_d) control the position of Tuzla Çayı and Sığırazmağı at the west of Tuzla (Figure A.43).

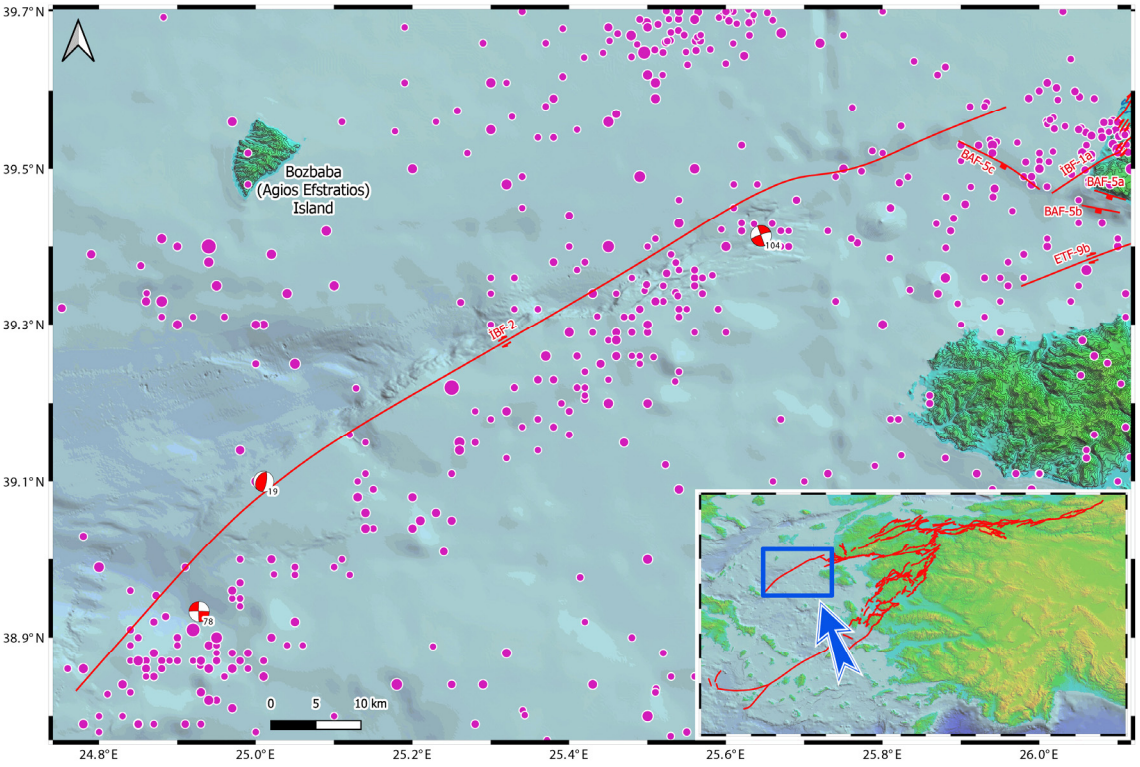

Figure A.44. The offshore continuation of İskiri-Biga Fault (İBF) and its relationship with the Babakale Fault (BAF) and Edremit Fault (ETF). Fuchsia dots with white circles are the epicenter locations of earthquakes (1900-2020, M≥3.5) from KOERI catalogue. For the focal mechanism solutions see Appendix B. See previous studies (Yaltırak et al., 2012; Emre et al., 2013; 2018) for comparison.

Details of the Balıkesir-Kepsut Fault (BKF)

One of the prominent morphological evidence for the Balıkesir-Kepsut Fault (BKF) is the right-lateral displacement (22.7 km) on Susurluk River (Figures 4 and A.45). It can be said that Susurluk River may follow the existing fault line (BKF-1a_d).

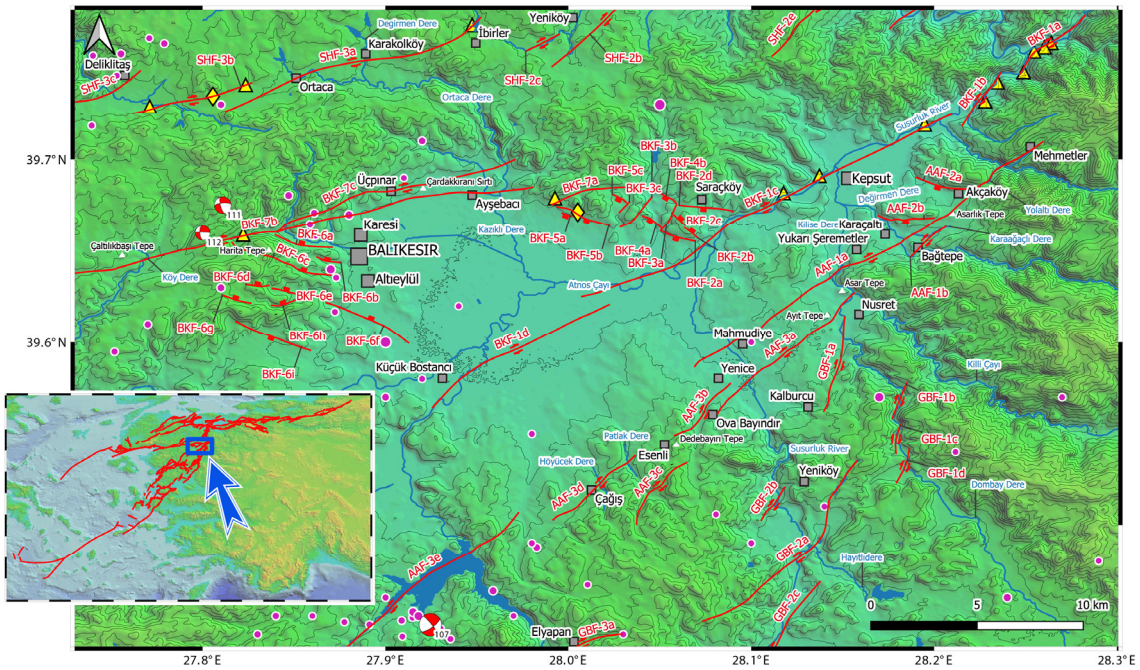

Figure A.45. The Balıkesir pull-apart basin and its surroundings. Fuchsia dots with white circles are the epicenter locations of earthquakes (1900-2020, M≥3.5) from KOERI catalogue. For the focal mechanism solutions see Appendix B. Yellow rhombic signs are paleoseismological trench locations from Sözbilir et al. (2016b). The yellow triangles represent the locations of structural data (Sümer et al., 2018; Seyitoğlu and Esat, 2022a). See previous studies (Emre et al., 2013; 2018; Seyitoğlu and Esat, 2022a) for comparison. SHF: Susurluk-Havran Fault; BKF: Balıkesir-Kepsut Fault; AAF: Akçaköy-Ataköy Fault; GBF: Gelenbe Fault.

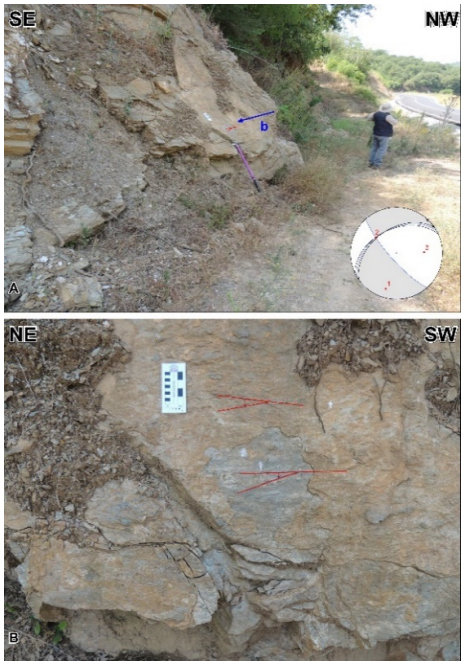

Figure A.46. A) Shear surface near to BKF-1a southwest Dereli. **B)** Close-up view of the kinematic data. The circle represents the equal area lower hemisphere spherical projection of the fault plane and slicken-lines. Gray and white areas (contractional and extensional areas, respectively) are the fault plane solution obtained by kinematic analysis of the fault data. The 1, 2, and 3 indicate the orientation of kinematic (strain) axes (after Seyitoğlu and Esat, 2022a).

Several fault surfaces are observed along the Susurluk River valley northeast and southwest of Kepsut (Seyitoğlu and Esat, 2022a). One of them is clearly seen in the southwest of Dereli (Figure A.46). Moreover, a right-lateral shift of 1800 m on the Nergis Çayı along the BKF-1d is measured at the east of Küçükbostancı (Figure A.45, Appendix C).

The normal faulted northeast margin of the Balıkesir pull-apart basin at the south of Akarsu and Saraçköy is bounded by the NW-SE trending, SW dipping BKF-2a, BKF-2d, BKF-4a_b and BKF-5a_c and their normal fault nature is proven by the paleoseismological study (Sözbilir et al., 2016b). Only the segments BKF-2b and BKF-2c are dipping NE. The NE-SW trending transfer faults are developed between these normal faults (Figure A.45). In the west of Balıkesir, WNW-ESE trending, NE dipping normal faults (BKF-6a_f) constitute the southwest margin of Balıkesir pull-apart basin. Only segment BKF-6i is dipping SW (Figure A.45).

The right-lateral strike-slip segments (BKF-7a_c) are located on the north of Balıkesir Plain. The BKF-7b creates 300 m right-lateral dislocation on the route of Kazıklı Dere at the east of Ayşebacı and continues to the south of Üçpınar where the elongated ridge, Çardakkıranı Sırtı, lies between BKF-7b and BKF-7c. Both segments continue to west and the BKF-7c merges to the BKF-7b at the west of Balıkesir at the north of Harita Tepe (Figure A.45). The BKF-7b creates a 250 m right-lateral diversion on the Köy Dere at the southeast of Çaltılıkbaşı Tepe. The right-lateral nature of the segment BKF-7b is also confirmed by the focal mechanisms of the seismic events #111_2020.08.29 (ML=3.7) and #112_2020.08.29 (ML=3.3) (Figure A.45; Appendices B and C).

Further to west-southwest, BKF-7b passes through Gökçeyazı (Figure A.47). In the northeast of İvrindi, the BKF-7b causes 1.6 km right-lateral diversion on the Koca Çay (Figure A.47). Additionally, anastomosing segment BKF-7d creates 1.8 km displacement on the Koca Çay. A total of 2.4 km right-lateral shift is measured along the segments of BKF-7b and BKF-7d. It is also noteworthy that a 250 m right-lateral shift is observed on the Göktepe Dere along BKF-7d (Figure A.47). Another important 1.8 km right-lateral displacement on Koca Çay occurs in the northwest of İvrindi along the BKF-7d which is getting close to the segment SHF4a of Susurluk-Havran Fault further west (Figure A.47, Appendix C).

Details of the Akçaköy-Ataköy Fault (AAF)

At the south of Kepsut, the NE-SW trending right-lateral Akçaköy-Ataköy Fault (AAF) is recognized mainly by using right-lateral diversions on the Değirmen Dere, Killi Çayı, Susurluk River, Patlak Dere and Nergis Çayı (Figures 4, A.45, and Appendix C). The segment AAF-1a is located on the linear Meşeyatağı and Yolaltı Dere between Mehmetler and Akçaköy. The AAF-1a passes through at the west of Asarlık Tepe and creates 280 m right-lateral displacement on Değirmen Dere between Karaçaltı and Bağtepe village. Further to southwest, AAF-1a also right-laterally displaced the Kilise Dere (900 m) at the west of Yukarı Şerametler and the Susurluk River (350 m) at Mahmudiye (Figure A.45).

An en echelon segment AAF-1b controls the position of Karaağaçlı Dere and Değirmen Dere at Bağtepe village. The stepping topography between north of Akçaköy and Karaçaltı indicates the existence of nearly E-W trending, S dipping normal faults (AAF-2a_b) (Figure A.45).

The northeast end of AAF-3a follows southeast slopes of Asar Tepe and Ayıt Tepe and controls the flow of Dombay Dere at the northwest of Nusret. The AAF-3a creates a 625 m right-lateral displacement on the Susurluk River at the south of Mahmudiye and terminates in the east of Ovabayındır (Figure A.45). The en echelon segment (AAF-3b) starts at the west of Yenice and follows the linear valley towards southwest and ends in the Esenli. In the south of Esenli, the AAF-3c mainly follows linear valleys creating a restraining stepover with the AAF-3b and Dedebayırı Tepe can be interpreted as pressure ridge at the west of Esenli. The en echelon segment AAF-3d is passing through in the Çağış and has 120 m and 200 m right-lateral dislocations on Patlak Dere and Höyücek Dere, respectively (Figure A.45).

The right stepping AAF-3e, which is located on the linear valley of Koca Dere, creates 1.5 km right-lateral displacement on the route of Kille Çayı. The focal mechanism solution of the seismic event #107_2019.12.10 (ML=5.0) indicates NE-SW trending right-lateral strike-slip faulting which can be correlated with the segment AAF-3e. The en echelon segments (AAF-4a_b) follow mainly the route of Koca Dere (Figures A.45, A.47; Appendices B and C).

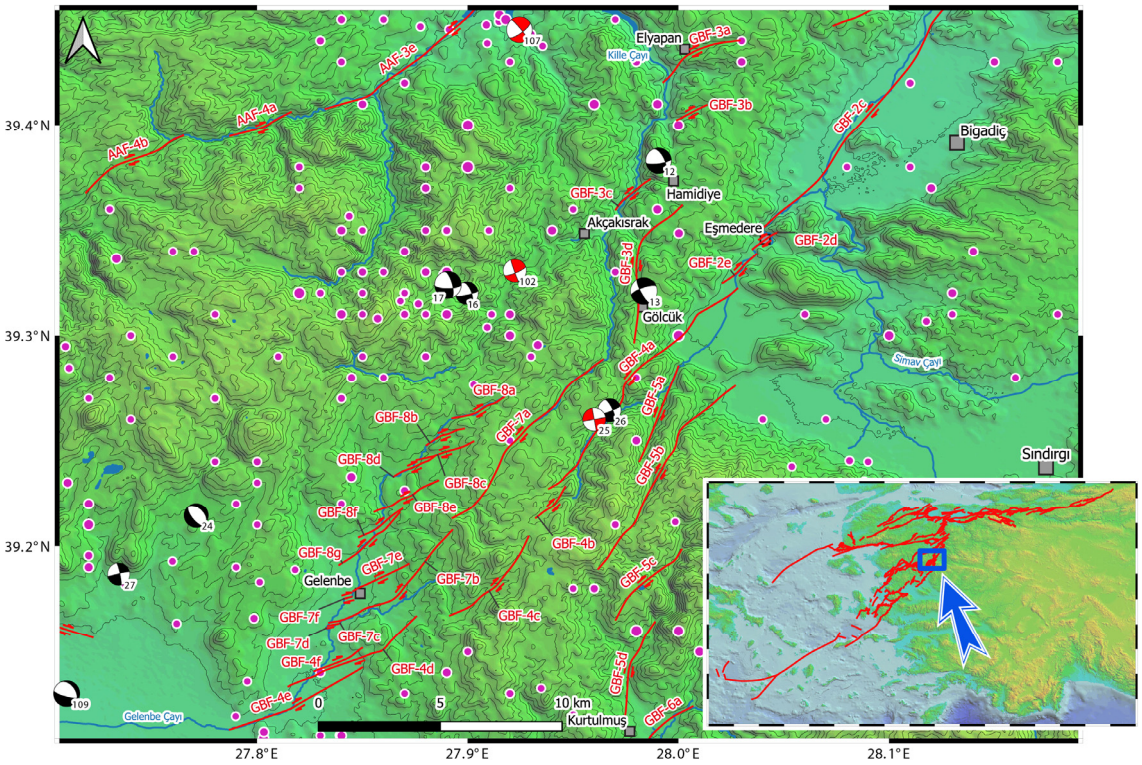

Figure A.47. The active faults between Bigadiç and Kurtulmuş. Fuchsia dots with white circles are the epicenter locations of earthquakes (1900-2020, M≥3.5) from KOERI catalogue. For the focal mechanism solutions see Appendix B. See previous studies (Emre et al., 2013; 2018) for comparison. AAF: Akçaköy-Ataköy Fault; GBF: Gelenbe Fault.

Details of the Gelenbe Fault (GBF)

The NNE-SSW trending Gelenbe Fault (GBF) was mapped as right-lateral strike-slip fault by Şaroğlu *et al*. (1992) and Emre *et al*. (2011a). The previous name is preserved but our segment distribution is quite different (Figure 4).

The GBF-1a creates 1380 m right-lateral offset on the route of Dombay Dere at the west of Nusret and reaches to the west of Kalburcu by following the linear valleys. The en echelon segments (GBF-1b_d) causes right-lateral displacements ranging 1.7 km to 630 m on the Dombay Dere (Figure A.45, Appendix C).

In the east of Yeniköy, the linear valley of Kaşıkçıpınar Dere hosts GBF-2a which displaces Simav Çayı 1170 m right-laterally. The GBF-2b is responsible for the 630 m right-lateral displacement on the Susurluk River (Simav Çayı) at the southwest of

Yeniköy (Figure A.45). There is a restraining offset between the GBF-2a and GBF-2c, probably for this reason, the sedimentary layers of Bigadiç Neogene basin are deformed in this area (Taşgın et al., 2018). The total right-lateral diversion of the Simav Çayı along the GBF-2a and GBF-2c in Bigadiç Plain reaches to the 15 km (Figures A.45, and A.47). The NNE-SSW trending two en echelon segments (GBF-2d_e) cause right-lateral diversions on the course of Eğri Dere at the south of Eşmedere village. Further to north-northwest, between Elyapan and Akçakısrak, three en echelon segments are located on the NE-SW trending linear valleys (GBF-3a_c). The segment GBF-3d is turning from NE to N-S direction between Hamidiye and Gölcük villages as drawn by Emre et al. (2011b). Between these segments, the seismic events #12_1999.07.24 (Mw=5.0) and #13_1999.07.25 (Mw=5.2) indicate right-lateral strike-slip faulting (Figure A.47, Appendix B). The GBF-4a_c and GBF-5a_d somewhat correspond to the Gelenbe Fault Zone of Emre et al. (2011a) but our segments have NNE-SSW trend rather than N-S continuous lines. Our trend is supported by the focal mechanism solution of the seismic event #26_2004.12.02 (Mw=4.5). Especially, the segments in the Gelenbe Plain (GBF-4d_f) have prominent NE-SW trends that is documented by right-lateral diversions on the course of Gelenbe Çayı (Figure A.47, Appendix B).

The Gelenbe Fault (GBF) reaches Kırkağaç Plain by GBF-4e and to the Akhisar Plain with the segments GBF-6a_b which are mainly located in the Gürdük Dere valley where 435 m right-lateral diversion on Kurtulmuş Çayı is measured at the west of Kurtulmuş village (Figure A.48). The Kışla Dere, a tributary of Gürdük Dere is shifted 540 m right-laterally at the west of Muştular along the GBF-6b. The en echelon segments of GBF-6c_h control the drainage in the Akhisar Plain and several right-lateral displacements ranging from 4.5 km to 1.4 km occur along the segments

between Akhisar and Saruhanlı (see also Tirkeş Fault of Özkaymak et al., 2013 for comparison) (Figure A.48).

Further to north, the segments (GBF-7a_f) are semi-parallel to the GBF-4a_f and create similar right-lateral displacements on the course of Gelenbe Çayı around Gelenbe town. The GBF-8a_g have generally short, NE-SW trending segments which are responsible for the right-lateral displacements on the Taşpınar Dere (140 m), Çobanlar Dere (460 m) and Koca Çay (100 m, 420m, 1200 m) at the north of Gelenbe town (Figure A.47). Majority of the focal mechanism solutions of the seismic events, further north (i.e., #102_2019.05.12, ML=4.5; #16_2001.05.24, Mw=4.4; #17_2001.06.22, Mw=5.2) support NE-SW trending right-lateral faulting in the area (Figure A.47, Appendix B).

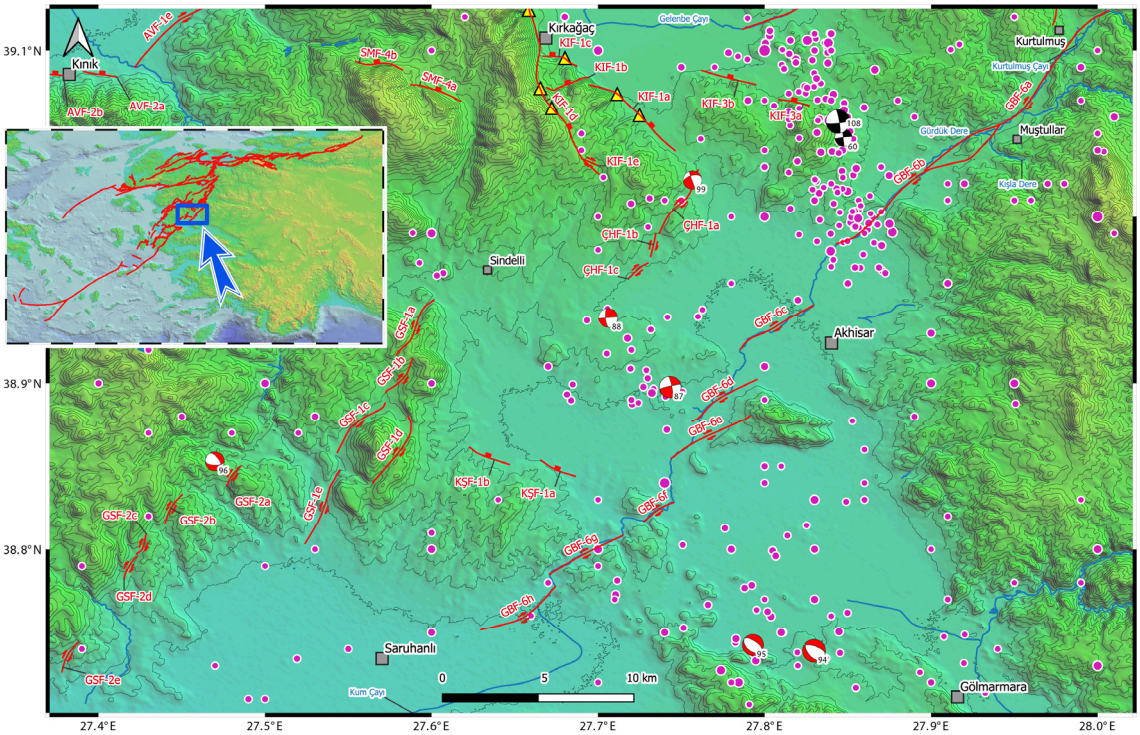

Figure A.48. The active faults between Akhisar and Kırkağaç. Fuchsia dots with white circles are the epicenter locations of earthquakes (1900-2020, M≥3.5) from KOERI catalogue. For the focal mechanism solutions see Appendix B. The yellow triangles indicate structural data locations of Uzel (2016). See previous studies (Uzel and Sözbilir, 2008; Emre et al., 2013; 2018; Uzel et al., 2013; Uzel, 2016) for comparison. GBF: Gelenbe Fault; KIF: Kırkağaç Fault; KŞF: Kayışlar Fault; GSF: Gülbahçe-Seyitoba Fault; SMF: Soma Fault.

Details of the Soma Fault (SMF) and Kırkağaç Fault (KIF)

The segments of Soma Fault (SMF) are located on the northwest and southeast of Soma town (Figure 4). The segments (SMF-1a_f; SMF-3a_g; SMF-4a_b) are the WNW-ESE trending, NE dipping normal faults in the southeast of Soma and drawn by using the topographic differences that is observed in between the Pre-Neogene basement and Neogene deposits and in the boundaries of the Quaternary deposits. The segments in the northeast of Soma town are NW-SE trending, SW dipping normal faults (SMF-2a_e) (Figure A.49, Appendix C).

The Kırkağaç Fault (KIF) shows normal fault character (KIF-1a_e; KIF-3a_b). The segments KIF-2a_b are evaluated as strike-slip faults with normal component (Uzel, 2016) (Figures A.47 and A.48).

The focal mechanism solutions of the #108_2020.01.22 (Mw=5.5) Musalar-Akhisar earthquake and its aftershock #109_2020.01.28 (Mw=4.9) together with the distribution of the numerous aftershocks indicate NNW-SSE trending left-lateral strike-slip and NW-SE trending normal faults, respectively (Figure A.48, Appendix B).

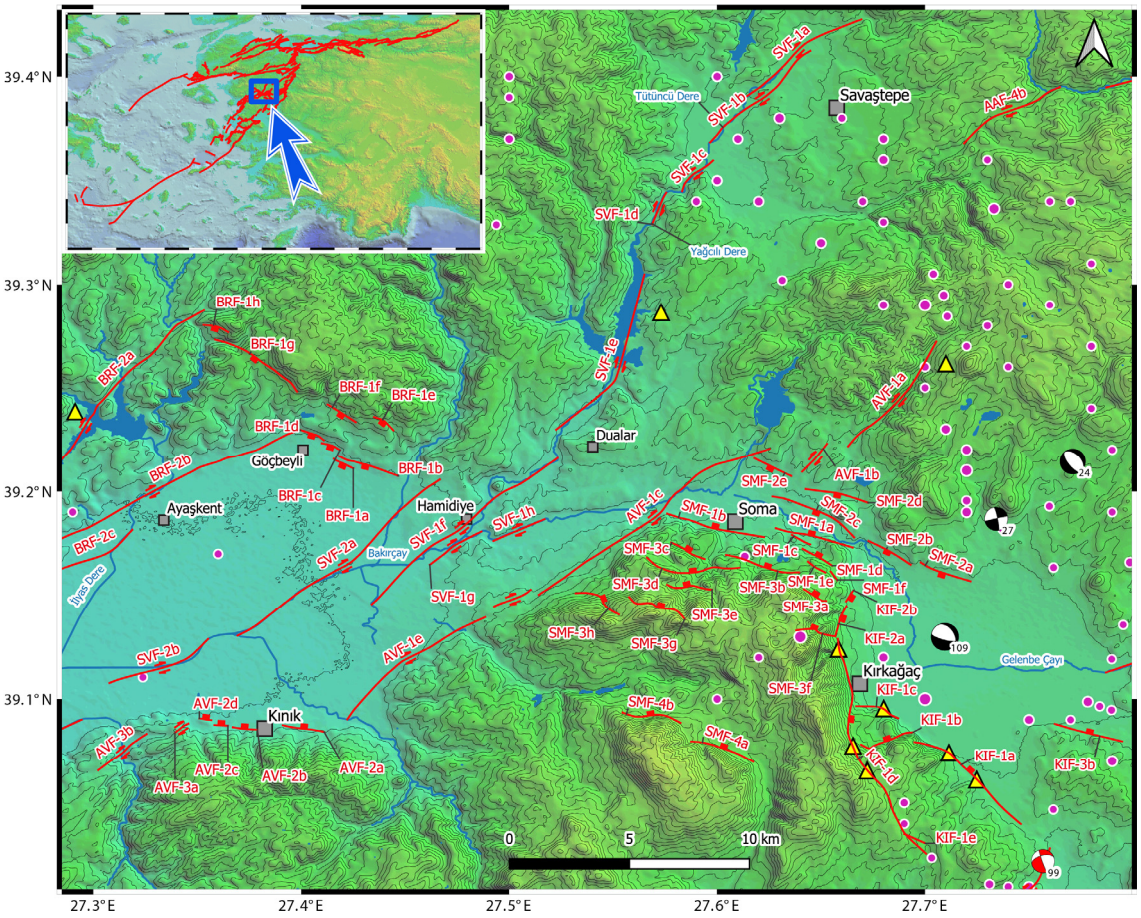

Figure A.49. The active faults between Savaştepe, Kınık and Kırkağaç. Fuchsia dots with white circles are the epicenter locations of earthquakes (1900-2020, M≥3.5) from KOERI catalogue. For the focal mechanism solutions see Appendix B. The yellow triangles indicate structural data locations of Uzel (2016) and Sangu et al. (2020). See previous studies (Uzel and Sözbilir, 2008; Emre et al., 2013; 2018; Uzel et al., 2013; Uzel, 2016) for comparison. SVF: Savaştepe Fault; BRF: Bergama Fault; AVF: Avdan Fault; SMF: Soma Fault; KIF: Kırkağaç Fault.

Details of the Avdan Fault (AVF) and Savaştepe Fault (SVF)

In the northeast of Soma, the linear valleys host the segments of Avdan Fault (AVF-1a_f). Their southwest continuation is located mountain-piedmont junction between the Köse Dağı and Bergama Plain (AVF-1c_e). The right stepping segments (AVF-3a_b) cause the formation of WNW-ESE trending, NE dipping normal faults in Kınık (AVF-2a_d) which is located on a releasing stepover (Figure A.49, Appendix C). The Savaştepe town is also located on a releasing offset between Savaştepe Fault (SVF) and Akçaköy-Ataköy Fault (AAF) (Figure 4). A 1.30 km right-lateral displacement on Tütüncü Dere along the SVF-1b and a 715 m right-lateral shift on the course of Yağcılı

Dere along the SVF-1c are measured. The routes of Yağcılı Dere and Bakırçay is controlled by the SVF-1f_h that caused sharp bending of the streams. It can be said that SVF-1f creates a total of 8.5 km right-lateral diversion on the route of Yağcılı Dere (including Bakırçay) around Hamidiye and Dualar (Figure A.49). The en echelon segments (SVF-2a_b) mainly control the position of Bakırçay in the Bergama Plain and the Savaştape Fault (SVF) reaches to Maruflar with the en echelon segments (SVF-2c_f) causing right-lateral diversions on the route of Koca Dere increasing from north to south (i.e., SVF-2c: 145 m; SVF-2d: 645 m; SVF-2e: 1000 m) (Figure A.50, Appendix C).

The Bergama Fault (BRF) is re-defined between north of Göçbeyli and Çandarlı via Bergama. It is mainly composed of the NE-SW trending right-lateral strike-slip segments and the NW-SE trending normal fault segments developed in the releasing offsets between the strike-slip segments (Figure 4, Appendix C).

In the northeast of Göçbeyli, NW-SE trending, SW dipping normal fault segments (BRF-1a_h) are developed in the releasing offset between the NE-SW right-lateral strike-slip faults of SVF and BRF-2a_b (Figure A.49). The strike-slip character of BRF-2b is determined by the 1.75 km right-lateral displacement on the İlyas Dere at the north of Ayaşkent. Moreover, semi-parallel BRF-2c causes 1.57 km and 1.25 km right-lateral shifting on the İlyas Dere and on the unnamed creek at the southwest of Ayaşkent, respectively (Figure A.49). All morphological evidences indicate that the structure known as Bergama Graben in the literature is in fact a structure controlled by strike-slip faulting (Figure 4).

The right stepping BRF-4a forms a releasing offset with the BRF-2c where the NW-SE trending, SW dipping normal fault (BRF-3) are developed at the northeast of

Bergama (Figure A.50). In the south of Bergama, the BRF-5a controls the position of Bakırçay and the southwest bending of Bergama Dere at the northeast of Sindel, indicating a right-lateral movement on the BRF-5a. The en echelon segments (BRF-5b_h) reach to the east of Çandarlı (Figure A.30). In the south of Ovacık, all fault lines bending to southwest. This is not only valid for the segments that show the right-lateral displacements (BRF-6a: 3.5 km; BRF-6b: 840 m and 340 m; BRF-6d: 270 m; BRF-6e: 540 m), but also observable for the semi-parallel, en echelon faults (SVF-2c_f; BRF-5b_h) (Figure A.50).

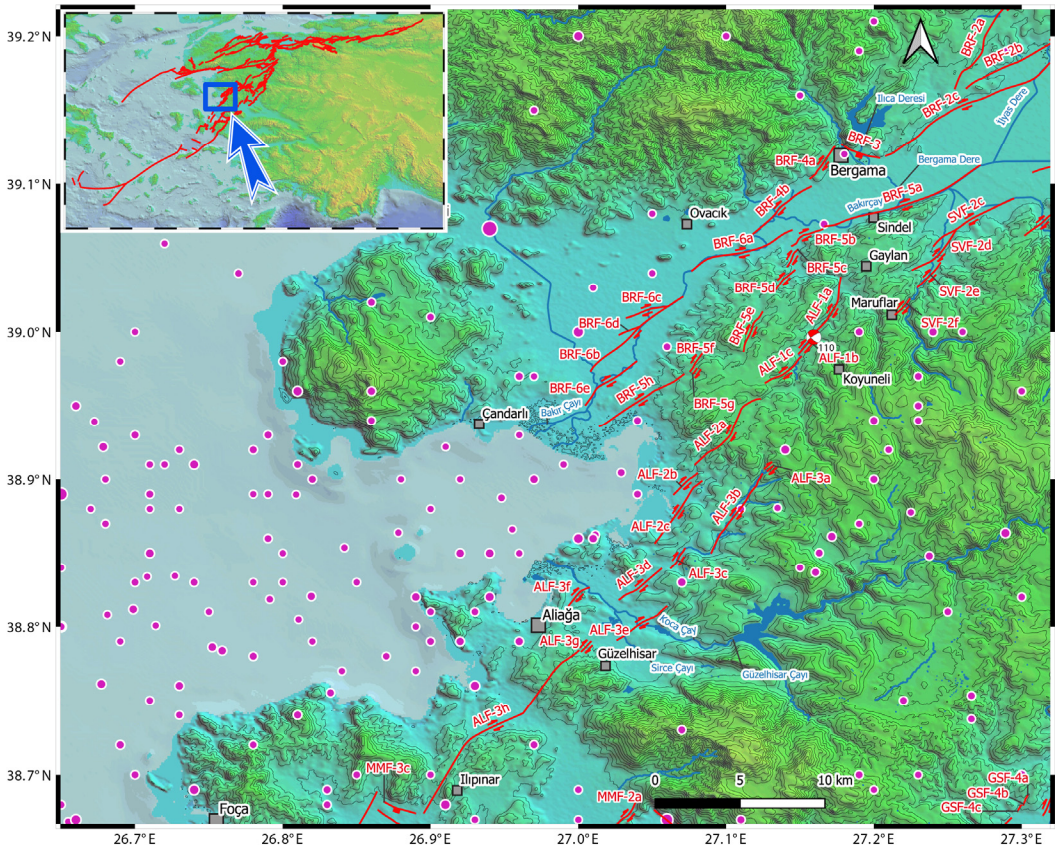

Figure A.50. The active faults between Bergama and Aliağa. Fuchsia dots with white circles are the epicenter locations of earthquakes (1900-2020, M≥3.5) from KOERI catalogue. For the focal mechanism solutions see Appendix B. See previous studies (Emre et al., 2013; 2018) for comparison. SVF: Savaştepe Fault; BRF: Bergama Fault; ALF: Aliağa Fault; MMF: Menemen Fault.

Details of the Aliağa Fault (ALF)

The Aliağa Fault (ALF) is lying between Gaylan and Ilıpınar via Aliağa having en echelon segments (ALF-1a_c; ALF-2a_c; ALF-3a_h). A 760 m right-lateral displacement is measured on the Kestel Dere along the segment ALF-1c at the west of Koyuneli where the seismic event #110_2020.08.14 (ML=3.0) provide strike-slip related focal mechanism solution. The segment ALF-3e creates right-lateral diversions of 400 m and 430 m on the course of Koca Çay and Sirce Çayı respectively in the Oyarda Plain at the north of Güzelhisar (Figure A.50; Appendices B and C).

Details of Çobanhasan Fault (ÇHF) and Kayışlar Fault (KŞF)

The position of Gelenbe Fault (GBF) was discussed in the Akhisar Plain (see above). The Çobanhasan Fault (ÇHF) is located on the western margin of Akhisar Plain and limits the Kırkağaç Fault (Figure 4). The NW-SE trending, NE dipping normal fault segments of Kayışlar Fault (KŞF-1a_b) seem to be developed in the releasing stepover between GBF and Gülbahçe-Seyitoba Fault (GSF) (Figure A.48). In the west of Akhisar Plain, the GSF is located between the south of Sindelli and Ayvacık villages (GSF-1a_e; GSF-2a_e; GSF-3a_d; GSF-4a_f) (Figure A.48, Appendix C).

Details of the faults between Manisa and İzmir

In the northwest of Manisa, Emre et al. (2011c) mapped left-lateral strike-slip faults (i.e., Muradiye Fault), but they are in the same direction with the right-lateral regional faulting (i.e., Gelenbe Fault) (Figure 5). The right stepping en echelon segments of Gülbahçe-Seyitoba Fault (GSF-4a_f) control route of the Gediz River (Figure A.51). This right stepping NE-SW trending fault segments are systematically observed between Manisa and Foça (GSF-4a_f; KLF-1a_g; MMF-2a_b; FYF-1a). Among these

stepping strike-slip faults, NW-SE trending normal faults are developed (KLF-2a_b; MMF-1a_b, MMF-3a_c) (Figures A.51 and A.52).

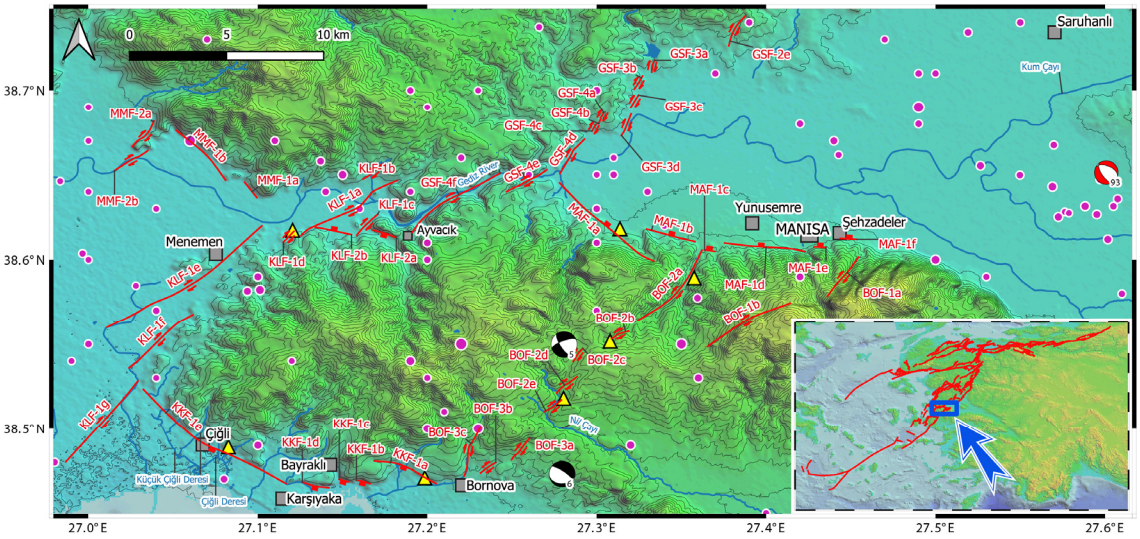

Figure A.51. The active faults between Manisa, Menemen and Bornova. Fuchsia dots with white circles are the epicenter locations of earthquakes (1900-2020, M≥3.5) from KOERI catalogue. For the focal mechanism solutions see Appendix B. Yellow triangles are the locations of structural data from Sözbilir et al. (2008), Uzel et al. (2012; 2013), Özkaymak et al. (2013). See also Emre et al. (2013; 2018) for comparison. GSF: Gülbahçe-Seyitoba Fault, MMF: Menemen Fault; KLF: Kubilay Fault; MAF: Manisa Fault; BOF: Bornova Fault; KKF: Karşıyaka Fault.

In this area, we understand that NE-SW trending faults have right-lateral strike-slip character (Figure 5), because NW-SE trending Menemen Fault (MMF) was reported as a SW dipping normal fault (Emre et al., 2011c). Otherwise, the MMF would beexpected to work as a reverse fault. For this reason, left-lateral strike-slip faults mapped in the northwest of Manisa (Emre et al., 2011c) is doubtful.

A similar structural style is observed in the south of Manisa where NW-SE and E-W trending normal fault segments (MAF-1a_f) of Manisa Fault are located in a releasing stepover between NE-SW trending right-lateral strike-slip fault segments of Bornova Fault (BOF-1a_b; BOF-2a_e; BOF-3a_c) and that of Gülbahçe-Seyitoba Fault (GSF-2a_e; GSF-a_d; GSF-4a_f) (Figure A.51).

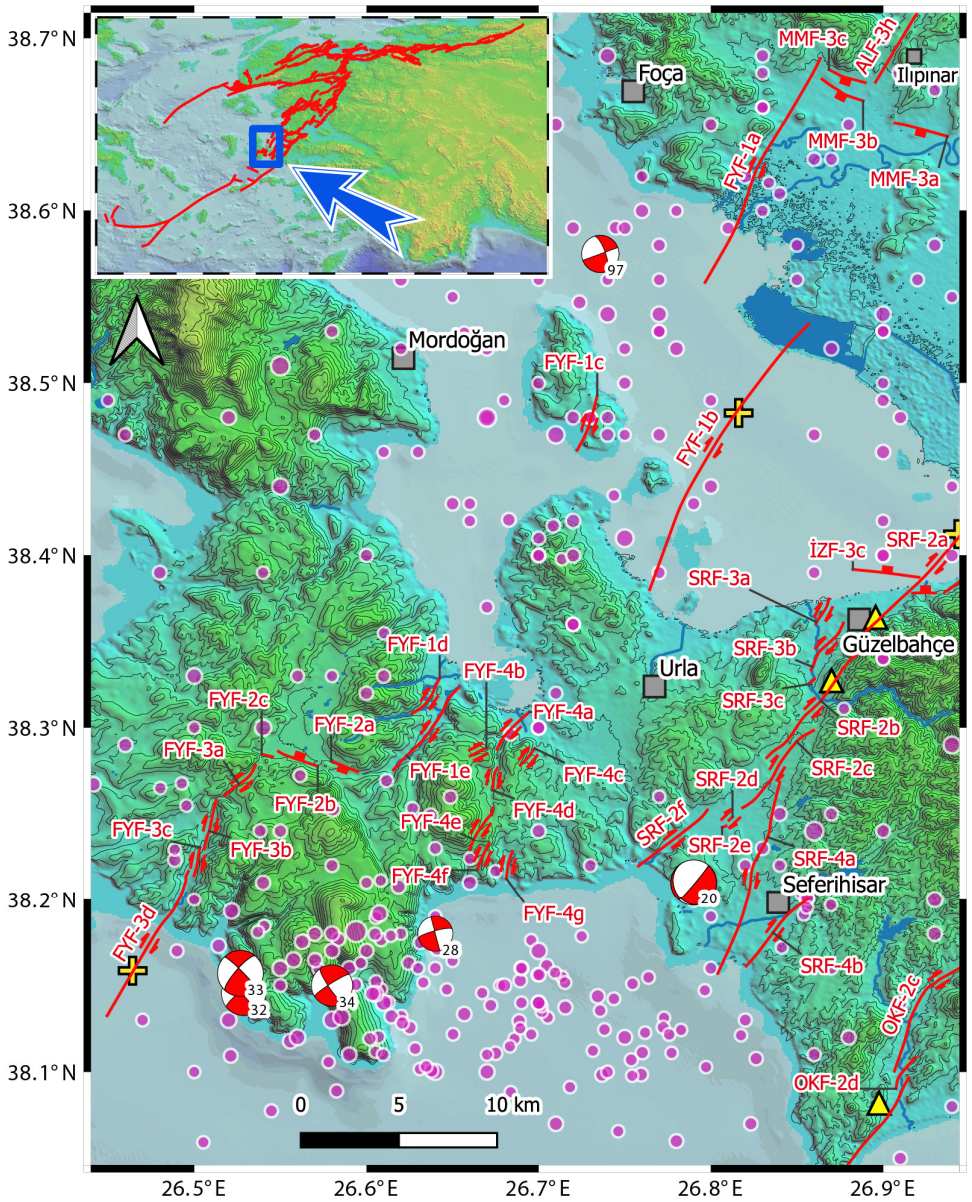

Figure A.52. The active faults between Foça and Seferihisar. Fuchsia dots with white circles are the epicenter locations of earthquakes (1900-2020, M≥3.5) from KOERI catalogue. For the focal mechanism solutions see Appendix B. Yellow triangles are the locations of the structural data from Sözbilir et al. (2008) and Uzel and Sözbilir (2008). Yellow plus signs are the locations of seismic reflection data from Ocakoğlu et al. (2005). See also previous studies (Uzel et al., 2012; Özkaymak et al., 2013; Emre et al., 2013; 2018) for comparison. ALF: Aliağa Fault; MMF: Menemen Fault; FYF: Foça-Yağcılar Fault; SRF: Seferihisar Fault; OKF: Orhanlı-Karabağlar Fault.

Details of the faults around İzmir Bay area

It is possible to evaluate the active faults of İzmir Bay in the similar structural framework mentioned above (Figure 5). The normal faults in the north of İzmir Bay were drawn in the form of convex arc to the south (Sözbilir et al., 2008) and in the

south of İzmir Bay, the normal faults were mapped in the form of convex arc to the north (Sözbilir et al., 2008; Emre et al., 2011c; Uzel et al., 2012). However, when the morphology around İzmir is closely examined, NW-SE trending, SW dipping normal fault segments of Karşıyaka Fault (KKF-1a_e) and NW-SE trending, NE dipping normal fault segments of İzmir Fault (İZF-1a_c; İZF-2a_c; İZF-3a_c) can be identified in both northern and southern side of İzmir Bay (Figures A.51 and A.53). This fault network must be developed in a releasing stepovers between semi-parallel NE-SW right-lateral strike-slip faults of eastern (Bornova Fault: BOF and Orhanlı-Karabağlar Fault: OKF) and western (Kubilay Fault: KLF and Seferihisar Fault: SRF) branches in the regional scale (Figure 5). It should be particularly emphasized that the short segments of İzmir Fault are located on the releasing stepovers between the segments of Seferihisar Fault (SRF-1a_d) in detail (Figure A.53). The focal mechanism solutions obtained from the seismic events #5_1974.02.01 (Mw=5.6) in Figure A.51 and #103_2019.08.08 (ML=5.0), #84_2015.01.10 (ML=4.3), #21_2003.04.17 (Mw=5.2) in Figure A.53 clearly indicates that the BOF and OKF are strike-slip character and they can produce a right-lateral shear zone with the SRF and KLF. Within this shear zone, the normal faults of KKF and İZF are developed (Figure 5).

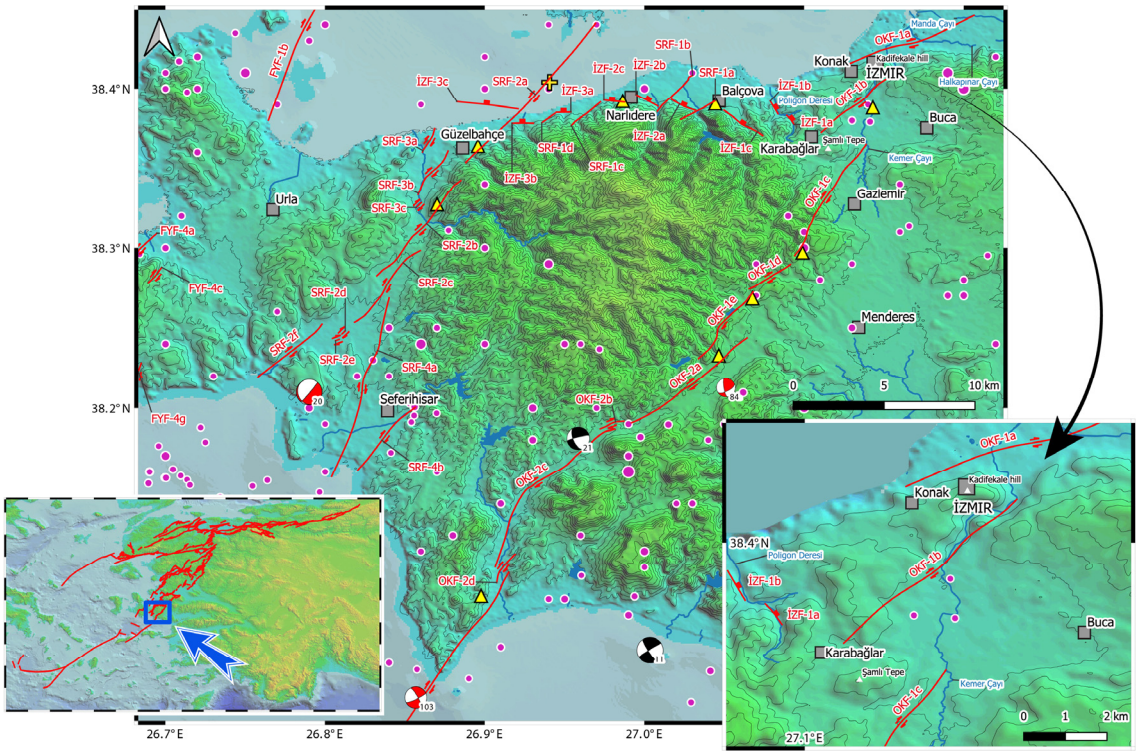

Figure A.53. The active faults between İzmir and Seferihisar. Inset: The details of the Kadifekale and Şamlı Tepe pressure ridges. Fuchsia dots with white circles are the epicenter locations of earthquakes (1900-2020, M≥3.5) from KOERI catalogue. For the focal mechanism solutions see Appendix B. Yellow triangles are the locations of the structural data from Sözbilir et al. (2008) and Uzel and Sözbilir (2008). Yellow plus sign is the location of seismic reflection data from Ocakoğlu et al. (2005). See also previous studies (Uzel et al., 2012; Özkaymak et al., 2013; Emre et al., 2013; 2018) for comparison. FYF: Foça-Yağcılar Fault; SRF: Seferihisar Fault; OKF: Orhanlı-Karabağlar Fault; İZF: İzmir Fault.

The Foça-Yağcılar Fault (FYF) is laying from Foça to Karaburun Peninsula (Figure 5). The seismic reflection sections in the İzmir Bay (Ocakoğlu et al., 2005) help to locate the segment FYF-1b (Figure A.52). Moreover, FYF-1d_e and FYF-3a_d create a releasing offset in which WNW-ESE trending normal fault segments (FYF-2a_c) are developed. The southwest continuation of FYF-3d is seen in the seismic reflection sections in the Zeytineli Bay (Ocakoğlu *et al*., 2005) (Figure A.32). The focal mechanism solutions of the seismic events #28_2005.01.29 (ML=4.5), #32_2005.10.17 (ML=5.7), #33_2005.10.17 (ML=5.9), #34_2005.10.17 (ML=5.3), #97_2017.12.25 (ML=4.8) clearly demonstrate that the FYF is a right-lateral strike-slip fault (Figure A.52; Appendices B and C).

The Orhanlı-Karabağlar Fault (OKF) is particularly important due to its northeast end locating in the city centre of İzmir (Figure 5). The segment OKF-1a is recognized by using the change of stream courses. These are the bend of Manda Çayı at Katipoğlu, the right bending of Halkapınar Çayı at Halkapınar and sharp right bending of Melez Çayı at Basmane which indicates right-lateral strike-slip character (Figure A.53). The OKF-1a is probably linked to the Bornova Fault (BOF). The en echelon segment OKF-1b creates a 2.77 km right-lateral displacement on the Kemer Çayı at the Hürriyet, Kadriye, Vezirağa districts of İzmir. The southwest continuation of OKF-1b reaches to the west of Şamlı Tepe. These segments should be tested by seismic reflection studies because they are passing in the highly populated area of İzmir. The en echelon OKF-1c is laying between east of Şamlı Tepe and southwest of Gaziemir (Figure A.53). It is interesting that the restraining offsets between the segments mentioned above, host the Kadifekale (hill) and Şamlı Tepe. They could be evaluated as pressure ridges which are, at the same time, active landslide areas (Ulamış and Kılıç, 2020; Kıncal et al., 2009). The landslide movements were reported after the 1778 earthquake in Kadifekale (Clarke, 1880) and the damage distribution of 1668 earthquake (Tepe et al., 2021) may be related to the position of segment OKF-1a rather than the İzmir Fault (Figure A.53 inset).

The southern continuation of right-lateral strike-slip Orhanlı-Karabağlar Fault (OKF-2e), which is confirmed by the focal mechanism solutions of the seismic events #103_2019.08.08 (ML=5.0), #39_ 2006.03.09 (ML=4.3), #75_2009.12.23 (ML=4.5) (Figure A.54, Appendix B). The recent seismic event of #113_2020.10.30 (Mww=7.0; USGS) Sisam (Samos) earthquake confirm the E-W trending north dipping normal fault at the north of Sisam (Samos) island (Caputo and Pavlides, 2013). It is interesting that some of the aftershocks of Sisam earthquake (i.e., #115_2020.10.30) shows NE-

SW trending right lateral strike-slip focal mechanism solutions. This enhance the position of segment OKF-2e in the offshore (Figure A.54, Appendix B).

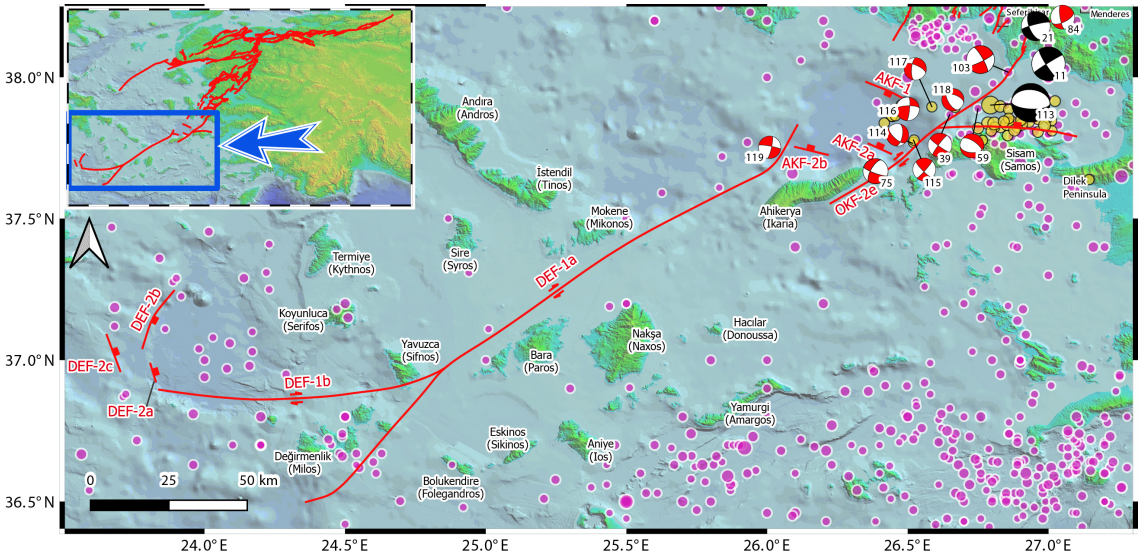

Figure A.54. The offshore continuation of the southern branch of NAFZ around Aegean islands. Fuchsia dots with white circles are the epicenter locations of earthquakes (1900-2020, M≥4) and yellow circles with black circles are recent seismic activity 2020.10.30 (Mww=7.0) Sisam (Samos) earthquake and its aftershocks (M≥4) from KOERI catalogue. For the focal mechanism solutions see Appendix B. See previous studies (Chatzipetros et al., 2013; Caputo and Pavlides, 2013; Philippon et al., 2014) for comparision. OKF: Orhanlı-Karabağlar Fault; AKF: Ahikerya Fault; DEF: Değirmenlik Fault.

Details of the Ahikerya Fault (AKF) and Değirmenlik Fault (DEF)

The NW-SE trending normal fault segments of Ahikerya Fault (AKF-1; AKF-2a_b) are drawn by using bathymetry map of Chatzipetros et al. (2013) and supported by the focal mechanism solutions of recent seismic events, #114_2020.10.30 and #117_2020.10.31) (FigSure A.54, Appendix B). The depression in the northeast of Ahikerya (Ikaria) island is evaluated as a pull-apart basin (Figure 5). The other right-lateral strike-slip fault segments of Değirmenlik Fault (DEF-1a_b) creating this pull-apart basin are drawn after Philippon et al. (2014) and our interpretation is supported by the focal mechanism solution of #119_2020.11.06 (Figure A.54, Appendix B). The segments (DEF-1a_b) corresponds to the Main Cycladic Lineament (MCL) in the literature and it is responsible for the 50 km right-lateral displacement of the

detachment fault in the Cyclades (Philippon et al., 2014). The normal fault segments (DEF-2a_c) terminating this strike-slip fault are drawn by using bathymetric data (Figure 5, A.54).